Rate-Dependent Bifurcations and Isolating Blocks in Nonautonomous Systems

A THESIS
SUBMITTED TO THE FACULTY OF THE GRADUATE SCHOOL
OF THE UNIVERSITY OF MINNESOTA
BY

Jonathan Hahn

IN PARTIAL FULFILLMENT OF THE REQUIREMENTS
FOR THE DEGREE OF
DOCTOR OF PHILOSOPHY

Richard McGehee

September, 2017

Acknowledgements

First and foremost, I would like to thank my advisor, Richard McGehee, for his countless ideas and constant inspiration.

Thank you to the other mentors I have had throughout my time in college and graduate school, especially Helen Wong, Stephen Kennedy, and Eric Egge. I would not have started down this path if I had not been propelled by such brilliant and inspiring teachers.

So many friends and fellow graduate students have supported me during my time in school. I would like to thank Logan Weiss, Mike Clark, Peter Scheuermann, Hai Ngo, Leah Willemin, and Ana Rodenberg for all the enthusiasm and encouragement you have given me over the last five years. I must also especially thank Kate Meyer, Rebecca Hahn, Yuriko Vaughan, and Robert Kennedy for all your help and advice. Finally, thank you to my family—Rebecca, Ben, Matt, and my parents—who continue to be greatest source of love and guidance throughout my life.

Abstract

We examine rate-dependent tipping and the behavior of solutions to nonautonomous systems from a topological perspective. We analyze an example of a rate-dependent bifurcation in which steady solutions begin to spiral, yet remain in a bounded region around a moving equilibrium. This example motivates us to develop a theory of isolating blocks for invariant sets in nonautonomous systems. Our examination of these isolating blocks reveals that solutions in rate-dependent systems are structurally stable; the rate-dependent forcing may have some amount of noise while the underlying behavior of solutions to the system remains the same. We also find isolating blocks useful for placing bounds on critical values for rate-dependent tipping in nonautonomous systems. Finally, we introduce rate-dependent tipping for discrete maps.

Contents

List of Tables

List of Figures

Chapter 1

Introduction

Dynamical systems are used regularly to model both physical and abstract systems, most commonly in the form of a system of differential equations. In this paper we will examine dynamical systems from a topological perspective and illustrate the results using concrete examples. We study nonautonomous systems, in which the evolution of the current state depends not just on its own value, but also on the current time. Such systems appear frequently in physical applications where an external parameter is forced over time.

Recently, researchers have begun to study systems with rate-dependent tipping points. This phenomenon occurs in systems which exhibit an equilibrium for a range of parameter values, but when the parameter is changing too quickly over time, this equilibrium also moves too quickly and the state variable fails to follow along. Instead, it tips away into another regime of state-space. Some of this research has been motivated by climate and ecological models, where rapidly changing parameters (e.g. temperature, CO_2, precipitation) may result in drastic consequences.

The original motivation for this work, and the first example we will consider, is a system with fast/slow dynamics and rate-dependent behavior. Analysis of this system has been used in a model of the Earth's climate and drying peatlands. We find, at the tipping point, a topological change in the behavior of solutions as they begin to spiral around the moving equilibrium. This observation has motivated us to apply theory of topological dynamics to examine the changes in solutions of systems with rate-dependent tipping.

Topological dynamics deals with the study of flows on topological spaces, and has its roots in Poincaré's study of the Three Body Problem in the late 19th century. Poincaré was interested in, among other things, determining whether solutions to the Three Body Problem exist in which the all three orbits are bounded. In 1947, Ważewski made an important contribution to the field of topological dynamics with a paper *Sur un principe topologique de l'examen de l'allure asymptotique des intégrales des équations différentielles ordinaires* [31], which provides a method to determine the existence of bounded solutions while knowing the behavior of the system only on the boundary of a closed set. Ważewski's work has inspired many of the ideas in this paper.

The closed sets bounding the solutions are called isolating blocks, and they can tell us information about the invariant solutions inside, if there are any. Conley showed that isolating blocks are stable when a system is perturbed, and he used this property to develop the well-known Conley index for isolated invariant sets. In this paper, we propose a similar method to examine novel kinds of rate-dependent bifurcations. We develop a theory of isolating blocks in nonautonomous systems to show that invariant solutions (those which do not leave the isolating block) are also stable under nonautonomous perturbations. As a result, the qualitative behavior of solutions can persist through perturbations in the forcing of systems with rate-dependent tipping.

In the rest of this chapter, we will provide a short introduction to the theory of rate-dependent tipping, the Conley index, and Ważewski's method. In Chapter 2 we analyze the rate-dependent bifurcation exhibiting spiral solutions in a fast/slow system. A portion of the material in Chapter 2 is based on [15]. In Chapter 3, we develop some theory of isolating blocks in nonautonomous systems, in both discrete and continuous-time settings. In Chapter 4, we apply this theory to differential equations with nonautonomous forcing, revisiting the rate-dependent systems of Chapter 2. In Chapter 5, we extend the scope of rate-dependent bifurcations for time-dependent discrete maps.

1.1 Rate-Dependent Bifurcations

A bifurcation in an autonomous system is defined as a change in the limiting behavior of the system under the variation of a parameter: the change in stability or annihilation of an equilibrium point or the birth or death of a periodic orbit or other invariant set.

In a system with rate-dependent tipping, a parameter is varied over time, but (unlike a dynamic bifurcation) the system does not bifurcate due to the parameter crossing a critical value. Instead, it is the rate of the change in the parameter which causes a change in the limiting behavior of the system.

A dynamical system on a space X where we find rate-dependent tipping has the form

$$\dot{x} = f(x, \mu, \lambda) \tag{1.1}$$

where $x \in X$ is the state, $\mu \in \mathbb{R}^k$ are fixed parameters, and $\lambda \in \mathbb{R}^n$ are time-dependent parameters. For each fixed value of λ in some subset $\Lambda \subset \mathbb{R}^n$, the system has a stable equilibrium $x^*(\lambda)$. The parameter λ changes as a function of time, i.e. $\lambda = \lambda(rt)$, where r, the rate parameter, determines how quickly λ changes. For small values of r, the solution to

$$\dot{x} = f(x, \mu, \lambda(rt)) \tag{1.2}$$

stays close to, or tracks, the *quasi-static equilibrium*, $x^*(\lambda(rt))$. However, above a certain value of r, the solution $x(t)$ fails to track the equilibrium, and exhibits some other behavior.

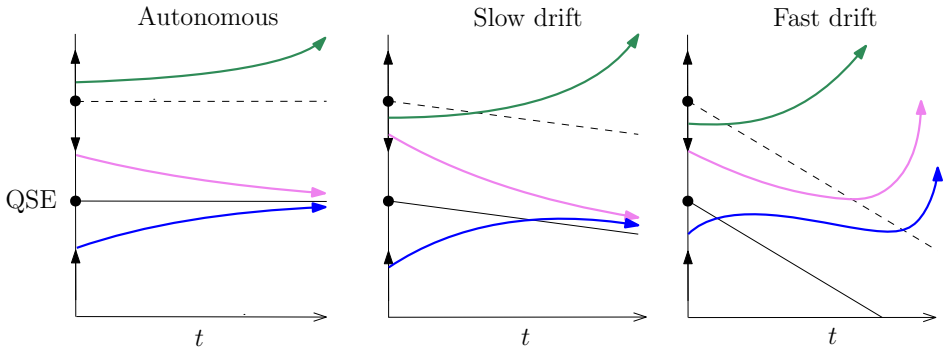

Figure 1.1: Rate-dependent tipping in a 1D system found in [2], with one stable equilibrium and one unstable equilibrium which are drifting steadily. For rates high enough, no solution can track the quasi-static equilibrium (solid line).

Many researchers have begun to study rate-dependent bifurcations, and how they differ from classical bifurcations, or bifurcations in the presence of noise. Notably,

Ashwin et al. [2], published a review which classified bifurcation-induced tipping, noise-induced tipping, and rate-induced tipping. Other authors have furthered this research, focusing on biasymptotic parameter shifts [1, 22, 32]. Many authors refer to the behavior as *rate-dependent tipping* or *rate-induced tipping*, as most systems studied involve a solution "tipping" away from an equilibrium. We use the phrase "rate-dependent bifurcation" to describe changes in the behavior of solutions more generally.

We take a more topological approach to the study of rate-dependent tipping than previous reserachers. We study the phenomenon not only to find critical rates at which solutions diverge from a moving equilibrium, but also to discover how the behavior of solutions change with the formation or destruction of invariant sets.

1.2 Autonomous and Nonautonomous Flows

If X is a Euclidean space, or more generally, a Riemannian manifold, an autonomous system is often described by a set of ordinary differential equations on X and an initial condition having the form

$$\dot{x} = f(x), \quad x(0) = x_0. \tag{1.3}$$

This contrasts with a nonautonomous system where the state evolution also depends on time:

$$\dot{x} = f(x,t), \quad x(0) = x_0. \tag{1.4}$$

When unique solutions to the autonomous system (1.3) exist, the family of solutions forms a *flow* on X. A flow is a continuous function $\phi : \mathbb{R} \times X \to X$; we often depict the flow by its time-t map $\phi^t : X \to X$ given by $\phi^t(x) = \phi(t,x)$. The time-t map of a flow is a homeomorphism which satisfies the group properties

$$\begin{aligned} \phi^0 &= \mathrm{id}_X \\ \phi^t \circ \phi^s &= \phi^{t+s}. \end{aligned} \tag{1.5}$$

The flow solves the initial value problem (1.3) if

$$\frac{d}{dt}\phi(t,x_0) = f(\phi(t,x_0)). \tag{1.6}$$

For a nonautonomous system (1.4), the set of solutions can be written as a function $\phi : \mathbb{R}\times\mathbb{R}\times X \to X$, where the family of maps $\phi(t,s) \coloneqq \phi(t,s,\cdot) : X \to X$ is characterized

by the properties

$$\begin{aligned} \phi(0,t) &= \mathrm{id}_X \\ \phi(t+s,r) &= \phi(t,s+r)\circ\phi(s,r). \end{aligned} \tag{1.7}$$

Alternatively, the function $\Phi : \mathbb{R}\times\mathbb{R}\times X \to \mathbb{R}\times X$ defined by

$$\Phi(t,s,x) = (t+s, \phi(t,s,x)) \tag{1.8}$$

is a flow on $\mathbb{R}\times X$. The curve $(t(\tau),x(\tau))$ in $\mathbb{R}\times X$ defined as $(t(\tau),x(\tau)) = \Phi(\tau,0,x_0)$ is a solution for the autonomous initial value problem where t is now a state variable:

$$\begin{aligned} \frac{d}{d\tau}t &= 1, & t(0) &= 0 \\ \frac{d}{d\tau}x &= f(x,t), & x(0) &= x_0. \end{aligned} \tag{1.9}$$

Nonautonomous dynamical systems can be defined more generally, where the state evolution does not depend directly on time, but on a separate autonomous dynamical system over a metric space P. In this framework we let θ^t be the time-t map of an autonomous flow on P. Suppose we have the continuous function $\varphi : \mathbb{R}\times P\times X \to X$, which defines the family of maps $\varphi(t,p) \coloneqq \varphi(t,p,\cdot) : X \to X$. Then (θ,φ) is a nonautonomous system if it satisfies the *cocycle property*:

$$\begin{aligned} \varphi(t,p) &= \mathrm{id}_X \\ \varphi(t+s,p) &= \varphi(t,\theta^s(p))\circ\varphi(s,p). \end{aligned} \tag{1.10}$$

To simplify matters, we will only let $P=\mathbb{R}$ and $\theta^t(p) = p+t$, which fits the framework of our nonautonomous flow.

1.3 Conley Index for Autonomous Flows

We give a brief overview of the Conley index in the setting of autonomous flows. To do this, we will need to define isolating neighborhoods and isolating invariant sets. A full introduction to the Conley index for flows can be found in several sources, for example [21, 9].

Definition 1. An *invariant set* for an autonomous flow ϕ, is a set S such that

$$\bigcup_{t\in\mathbb{R}} \phi(t,S) = S. \tag{1.11}$$

For a given set N, the *invariant set of* N is defined as

$$\mathrm{Inv}(N,\phi) \coloneqq \{x \in N | \bigcup_{t\in\mathbb{R}} \phi(t,x) \subset N\} \tag{1.12}$$

It is not difficult to show that $\mathrm{Inv}(N,\phi)$ is an invariant set.

Definition 2. A set N is an *isolating neighborhood* if $\mathrm{Inv}(N,\phi) \subset \mathrm{int}\ N$. We say an invariant set S is an *isolated invariant set* if there is an isolating neighborhood $N \supset S$ such that $\mathrm{Inv}(N,\phi) = S$.

An isolating block encompassing an invariant set has stricter conditions. Isolating blocks can be defined in multiple ways; we use the definition provided in [21]. Isolating blocks have invariant topological properties characterized by the Conley index. The Conley index is formed by a pair of sets which are, essentially, a compact isolating neighborhood of an invariant set S and the set of boundary points which flow out of the neighborhood.

Definition 3. A compact set B is an *isolating block* for S if the set of points which exit the block immediately,

$$B^- \coloneqq \{x \in B \mid \phi([0,T),x) \not\subset B \text{ for all } T > 0\}, \tag{1.13}$$

is closed and for all $T > 0$, the set of points with forward and backward trajectories that remain in B over the time interval $[-T,T]$,

$$\{x \in B \mid \phi([-T,T],x) \subset B\}, \tag{1.14}$$

lies in the interior of B. This condition excludes trajectories with internal tangencies in B.

Definition 4. A pair of compact sets (N,L) where $L \subset N \subset X$ is called an *index pair* for S if the three properties hold:

1. $N \setminus L$ is a neighborhood of S, and $S = \mathrm{Inv}(\mathrm{cl}(N \setminus L),\phi)$;
2. L is *positively invariant* in N; that is, for $x \in L$, if $\phi([0,t],x) \subset N$, then $\phi([0,t],x) \subset L$;

3. L is an *exit set* of N; that is, for $x \in N$, if $\phi(t, x) \notin N$, then for some $s \in [0, t]$, $\phi(s, x) \in L$ and $\phi([0, s] \subset N$.

For any isolated invariant set S of a flow, there exists an isolating block B of S and (B, B^-) is an index pair for S [21]. An example of an index pair is shown in Figure 1.2.

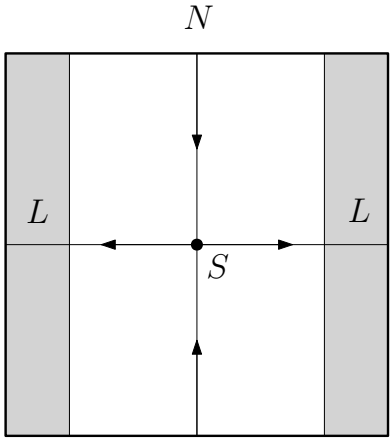

Figure 1.2: An autonomous index pair (N, L) surrounding a saddle equilibrium, S. Here N is the entire square and L consists of the two shaded sides.

1.3.1 Quotient Spaces, Pointed Spaces, and the Conley Index

Suppose that N is a topological space, and $L \subset N$. Let $[L]$ be the equivalence class of points in L under the equivalence relation $x \sim y$ if $x, y \in L$ or $x = y$. The quotient space N/L we will define as the space $(N \setminus L) \cup \{[L]\}$. A subset $U \subset N/L$ is open in N/L if $[L] \notin U$ and U is open in N, or $[L] \in U$ and $(U \cap (N \setminus L)) \cup L$ is open in N. This is equivalent to the usual definition of the quotient space $N/\sim$.

A topological pointed space, (X, x_0), consists of a topological space X and a distinguished point x_0. We will write N_L to mean the pointed quotient space $(N/L, [L])$, with the distinguished point $[L]$.

Definition 5. Let S be an isolated invariant set of a flow ϕ. The Conley Index, $I(S, \phi)$, is the collection of pointed spaces N_L where (N, L) is an index pair for S. The homotopy Conley index, $h(S, \phi)$, is defined as the homotopy type of the pointed space N_L.

The homotopy Conley index is well-defined, as for two index pairs (N, L) and $(\tilde{N}, \tilde{L})$ for the same invariant set S, the pointed spaces N_L and $\tilde{N}_{\tilde{L}}$ are homotopically equivalent. Two important properties the Conley index are

1. (Ważewski Property) Let $\bar{0}$ be the homotopy type of the pointed space $(\emptyset, \emptyset)$, the empty set with an empty set as the identified point. Let N be an isolating neighborhood, and let (N, L) be an index pair for $S = \text{Inv}(N, \phi)$. If $h(S, \phi) \neq \bar{0}$, then $S \neq \emptyset$.

2. (Continuation Property) Given a continuous family of flows ϕ_λ for $\lambda \in [0, 1]$, if N is an isolating neighborhood of the invariant set S_λ for each ϕ_λ in the family, then for $\lambda_1, \lambda_2 \in [0, 1]$, we say ϕ_{λ_1} and ϕ_{λ_2} are related by continuation. If ϕ_{λ_1} and ϕ_{λ_2} are related by continuation, $h(S_{\lambda_1}, \phi_{\lambda_1}) = h(S_{\lambda_2}, \phi_{\lambda_2})$.

The continuation property can be useful in finding the homotopy type of complicated flows, by relating the flow to a simpler one by continuation. The Ważewski property can be used to show the existence of invariant sets based on the flow on the boundary of a compact set, which is an equivalent restatement of Ważewski's Theorem. We discuss this theorem more in the next section.

1.4 Ważewski's Theorem for Nonautonomous Systems

The Conley index described in the last section applies to autonomous flows on compact spaces. A nonautonomous system on X as in (1.4) can be extended into an autonomous system on $\mathbb{R} \times X$ as in (1.9). However, with this framework all invariant solutions are unbounded in time, so a Conley index for compact spaces will not apply directly. Still, partial solutions bounded within compact sets in $\mathbb{R} \times X$ may have similar topological properties based on the exit sets of the bounding set. Ważewski's method can be applied to nonautonomous systems to discern properties of invariant sets based on the flow on the boundary of a region in $\mathbb{R} \times X$. A full introduction to Ważewski's method can be found in [29]. We provide a brief introduction here.

Let V be an open subset of the state-space of the system, X, and let $\phi : \mathbb{R} \times X \to X$ be a flow.

Definition 6. Let $x \in \partial V$ be a point on the boundary of V. We say x is an *egress point* of V if $\phi(t, x) \in V$ for $t \in (-\epsilon, 0)$ for some $\epsilon > 0$. The set of egress points we will denote E. If it also holds that $\phi(t, x) \in X \setminus V$ for $t \in (0, \epsilon)$, then x is a *strict egress point*.

Definition 7. A point $x \in V$ is an *escape point* if there exists a time $t > 0$ such that $\phi(t, x) \notin V$. The set of escape points of V we will denote V^*. The *escape time*, denoted $\sigma(x)$, is the positive time such that $\phi([0, \sigma(x)), x) \subset V$ and $\phi(\sigma(x), x) \in E$.

Theorem 8. *[Ważewski] Let $Y \subset E$ and let $Z \subset V \cup Y$. Suppose the following hypotheses hold:*

1. *All egress points $x \in E$ are strict egress points.*
2. *$Z \cap Y$ is a retract of Y.*
3. *$Z \cap Y$ is not a retract of Z.*

Then there exists a point $x \in Z$ such that either

1. *$\phi(\mathbb{R}^+, x) \subset V$ or*
2. *$x \in V^*$ and $\phi(\sigma(x), x) \in E \setminus Y$.*

Ważewski's theorem can be used to prove topological results about bounded solutions in nonautonomous systems, similar to the use of Conley's index for autonomous systems. As an example we describe a nonautonomous version of an unstable periodic orbit.

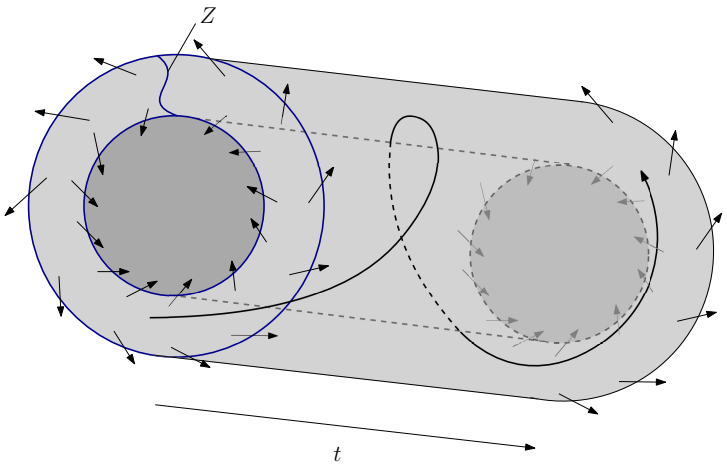

Figure 1.3: Invariant solution within an annular isolating neighborhood.

Example 9. [Annulus Invariant Set] Let $\phi : \mathbb{R} \times \mathbb{R} \times \mathbb{R}^2 \to \mathbb{R} \times \mathbb{R}^2$ be a flow on $\mathbb{R} \times \mathbb{R}^2$. Suppose that $V \in \mathbb{R} \times \mathbb{R}^2$ is the tubular region $\{(t, x, y) \mid a^2 < x^2 + y^2 < b^2\}$, with $a, b > 0$ as in Figure 1.3. Suppose that the set of egress points of V is the entire boundary: $E = \{(t, x, y) \mid x^2 + y^2 = a^2 \text{ or } x^2 + y^2 = b^2\}$, and suppose all egress points are strict. Let $Y = E$. Let Z be the union of Y and any continuous path in $V \cap (0 \times \mathbb{R}^2)$ (a path at time $t = 0$) from the inner ring of Y (radius a) to the outer ring (radius b).

Then $Z \cap Y$ is a retract of Y, but $Z \cap Y$ is not a retract of Z. Thus, by Ważewski's theorem, since $E \setminus Y = \emptyset$, there must be a point $(0, x, y)$ in $Z \setminus Y$ that has a positive trajectory contained in V. Hence, any path at $t = 0$ from the inner ring to the outer ring necessarily contains a point in the invariant set of V (and the invariant set is nonempty).

The autonomous version of this example is a flow on $V \subset \mathbb{R}^2$ where V is the annulus between a radius of a and b with the exit set V^- being the entire boundary. The homotopy index for (V, V^-) is the sum of a pointed one-sphere and a pointed two-sphere, which is the homotopy index of a periodic orbit with one positive Floquet exponent.

Although the Conley index may not apply to the nonautonomous system in this example, Ważewski's method nonetheless allows us to glean information about the invariant set. The tube V extends infinitely in time, so it is not compact and we cannot compute a Conley index. However, we know the invariant set is nonempty, and any path from the inner ring the outer ring of V intersects it.

Chapter 2

Hopf Bifurcations in Systems with Rate-Dependent Tipping

Simple examples have often facilitated the understanding of phenomena that may arise in more complex or general settings. Such is the case with the systems we analyze in this chapter, which feature rate-dependent tipping in fast/slow systems with an equilibrium near the fold of a critical manifiold. This system appeared in a paper by Ashwin et al. [2], in which the authors investigated representative examples for a general theory of rate-dependent tipping. Ashwin et al. used geometric singular perturbation (GSP) theory to determine a critical rate of tipping while a small parameter, ϵ, approached 0 in the fast/slow system. GSP is a powerful and often-used technique for analyzing fast/slow systems; however, we demonstrate that it may not give us a full understanding of the system for $\epsilon > 0$ in this case.

The example concerns a steadily moving *quasi-static equilibrium* (QSE) near the fold of a folded critical manifold in a 2-dimensional fast/slow system. The GSP analysis of Ashwin et al. provides a critical rate of tipping for $\epsilon \to 0$, which gives a good approximation for the value that determines when trajectories slip over the fold, tipping away from the equilibrium. This analysis gives the impression that there exists a rate-dependent bifurcation in this system where, at the critical rate, a globally stable equilibrium becomes a repelling equilibrium and all trajectories head toward infinity, or at least far away from the QSE. In actuality, however, for any fixed value of $\epsilon > 0$, none

of the solutions diverge to infinity.

We can perform a change of coordinates which reduces the system into an autonomous co-moving system in which the rate parameter is a standard bifurcation parameter. The index theory developed by Conley rules out the possibility for a single global attractor to disappear in this way.

We will show that the reduced system actually undergoes a Hopf bifurcation at the critical rate, and an asymptotically stable limit cycle is born from the destabilizing equilibrium. This limit cycle grows continuously, meaning that trajectories do not simply change from tracking an equilibrium to approaching infinity. The distance of the limit cycle from the equilibrium grows continuously with the rate parameter. The limit cycle grows quickly, which gives the impression of a tipping event, but it is still a continuous change. In the original (not co-moving) system, the bifurcation results in trajectories which spiral around the quasi-static equilibrium, rather than diverging away. As the rate parameter increases further, the limit cycle in the reduced system increases in size, and in the original system the orbits spiral with increasing amplitude. There is no immediate jump in the distance of trajectories from the moving equilibrium; rather, the maximum distance of solutions from the QSE grows continuously as the amplitude of their orbits increase. This makes the critical rate more of a "bifurcation point" than a "tipping" threshold.

The growing limit cycle in this system is actually an instance of a canard phenomenon, whose prototypical example is the van der Pol oscillator. In early days it was thought that the van der Pol system changed from having a stable equilibrium to a large limit cycle immediately upon bifurcation because that is what happened in numerical simulations. It is now known that the system actually goes through a transition where canard cycles continuously increase to the large limit cycle during a very small range of the bifurcation parameter. The same sort of canard phenomenon occurs in the fast/slow system that Ashwin et al. analyze.

The steady drift of the QSE allows for our convenient reduction into an autonomous system. This motivates the question of how we would analyze a system for which that reduction was not possible. In the following chapters, we provide some means to answer this, using theory of isolating blocks of invariant sets in nonautonomous systems. In particular, we will show that the spiraling invariant solutions are structurally stable;

they will exist even when the forcing function $\lambda(rt)$ is perturbed some amount and the system can no longer be reduced to an autonomous one. This one example provides motivation for the rest of this thesis, in which we seek to better understand the structure of rate-dependent bifurcations.

2.1 Rate-Induced Bifurcations

Bifurcations are conventionally viewed as changes in the stability or existence of an equilibrium or limit cycle as a parameter varies. Rate-dependent or rate-induced bifurcations differ from this convention in that the stability of a system does not change with the variation of a parameter; rather, a parameter varies too quickly for the state to follow the movement of an equilibrium point. In many examples of rate-dependent tipping, there exists a critical rate defining a threshold for the rate of change of the parameter. Below the critical rate, the state is able track the equilibrium, and past the critical rate the state fails to track it, and "tips."

Consider a system with state vector $x \in \mathbb{R}^n$, with parameters $\mu \in \mathbb{R}^k$ that do not vary over time, and a time-dependent external forcing function $\lambda(rt) \in \mathbb{R}^l$:

$$\frac{dx}{dt} = f(x, \mu, \lambda(rt)) \tag{2.1}$$

Here r is the rate of the forcing function. We will assume that for every fixed value of λ in some domain, the system has a stable equilibrium, $\tilde{x}$. We will also assume that the stable state depends continuously on λ. So the equilibrium of the system can be written as $\tilde{x}(\lambda)$. For small values of r, the state will track the moving equilibrium, $\tilde{x}(\lambda(rt))$, called the *quasi-static equilibrium* (QSE). For r large enough, it is possible that the quasi-static equilbrium moves too quickly for trajectories to follow. In this situation, we say there is a rate-dependent bifurcation.

Authors such as Perryman and Ashwin et al. [2, 1, 22] use various criteria to determine when a rate-induced tipping point has occured. They analyze some examples with a *tipping radius* R. The system tips if the state reaches a distance of R from the QSE. In other examples, there may be a topological change in the system which causes the state to move away from the QSE, perhaps to the basin of attraction of another equilibrium, as in [27]. Sometimes, as in [32], tipping is said to occur when an excursion

happens due to the formation of a canard trajectory. The criterion for tipping can be prescribed arbitrarily, or it can depend on a physical meaning rather than topological properties of the system. In the examples we consider, the natural criteria for a tipping threshold is a topological change in the system which causes the solutions to diverge from the QSE.

We will look at three fast-slow systems which have a rate-induced bifurcation phenomenon. First we examine the system that appeared in [2]. Next we analyze a system similar to the forced van der Pol oscillator in [14] where the same rate-tipping phenomenon occurs. The canard explosion in the unforced van der Pol system is well-established. Lastly, we investigate the Rosenzweig-MacArthur model of consumer dynamics in ecology. Each of these examples have a steadily drifting stable equilibrium near a fold. Weiczorek et al. [32] also analyze fast/slow systems with a stable equilibrium near the fold of a critical manifold. However, Weiczorek et al. study behavior with a logistic forcing function, while our analysis is concerned with constant linear forcing.

2.2 Fast/Slow System with Rate-Dependent Tipping

This section concerns a two-dimensional fast-slow system with a linear forcing function $\lambda(t) = rt$. Ashwin et al. analyze this system in the limit as the fast parameter ϵ goes to 0. They find a critical tipping point at $r_c = \sum_{n=1}^{N}(1/2)^n$. We further observe that when r exceeds this critical value, the state begins to spiral around the quasi-static equilibrium.

The fast-slow system in [2] (equations 3.12 - 3.14), with state variables (x, y) and forcing parameter λ increasing with rate r is given by

$$\begin{aligned} \epsilon\frac{dx}{dt} &= y + \lambda + x(x-1) \\ \frac{dy}{dt} &= -\sum_{n=1}^{N} x^n \\ \frac{d\lambda}{dt} &= r > 0 \end{aligned} \tag{2.2}$$

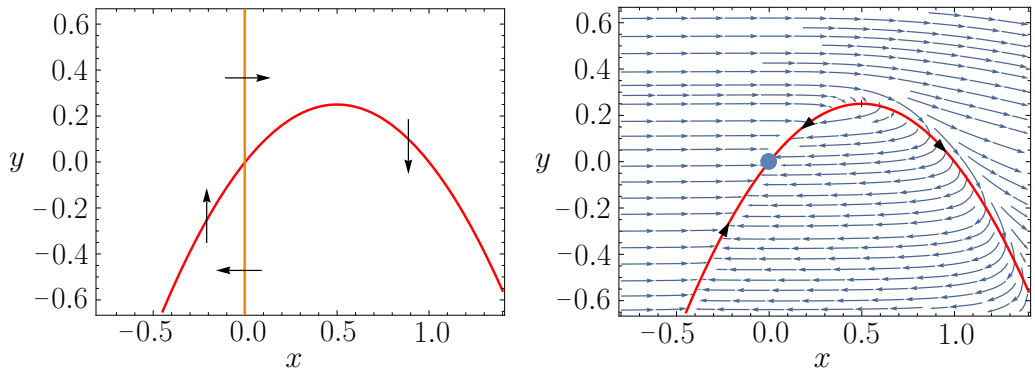

Figure 2.1: Left: Isoclines of the fast-slow system (2.2). Right: Phase portrait of the same system with a fixed $\lambda = 0$ and $\epsilon = .01$. The slow manifold is shown in red, and the dot shows the equilibrium point $(0, 0)$.

In this example N is odd and $N \geq 5$, which ensures a globally stable equilibrium at $(x = 0, y = -\lambda)$ with a fold at $(x = \frac{1}{2}, y = -\lambda + \frac{1}{4})$ for fixed λ. A phase portait of the system is shown in Figure 2.1. Three numerically computed trajectories with different behaviors are depicted in Figure 2.2.

2.2.1 Singular Perturbation Analysis

We will go through a brief summary of the analysis in Ashwin et al. [2] to find the critical rate for $\epsilon \to 0$. Fixing λ and setting $\epsilon = 0$ in the equation for $\frac{dx}{dt}$ gives the critical slow manifold as the set of points satisfying $0 = y + \lambda + x(x-1)$, which is a folded manifold with a fold point at $(x, y) = (\frac{1}{2}, -\lambda + \frac{1}{4})$. This manifold has an attracting part where $x < \frac{1}{2}$ and a repelling part where $x > \frac{1}{2}$. The slow dynamics on the critical manifold can be approximated by differentiating this expression with respect to t:

$$0 = \frac{dy}{dt} + \frac{d\lambda}{dt} + \frac{dx}{dt}(2x - 1) \tag{2.3}$$

Solving for $\frac{dx}{dt}$, the resulting dynamics of x on the critical manifold is governed by the equation

$$\frac{dx}{dt} = (\sum_{n=1}^{N} x^n - r)(2x - 1)^{-1} \tag{2.4}$$

The system is singular at $x = \frac{1}{2}$, but rescaling time with $\frac{dt}{d\tau} = -(2x-1)$, gives a desingularized equation for x, with time reversed for $x > \frac{1}{2}$:

$$\frac{dx}{d\tau} = r - \sum_{n=1}^{N} x^n. \tag{2.5}$$

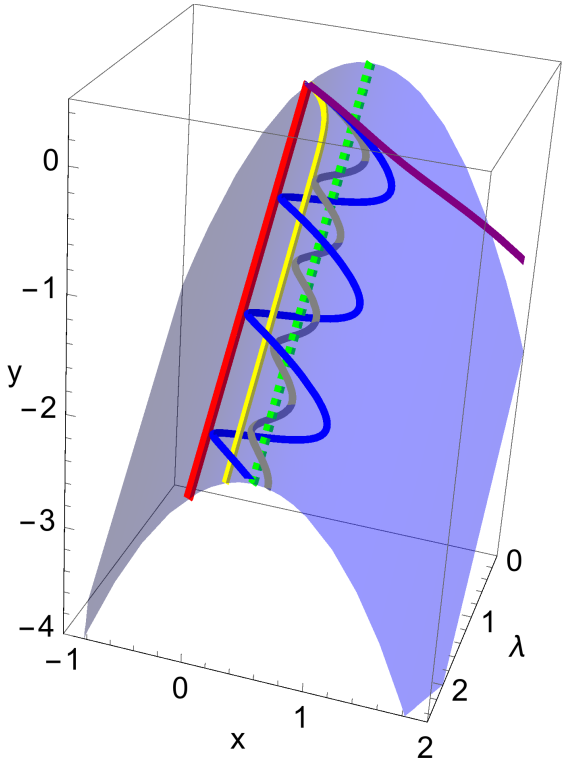

Figure 2.2: The critical manifold as a two-dimensional manifold in (x, y, λ). The QSE at $(0, -\lambda, \lambda)$ is plotted as a solid red line, and the fold of the critical manifold at $(1/2, -\lambda + 1/4, \lambda)$ is a dashed green line. Trajectories shown for various rates below r_c (steady) and above r_c (spiraling).

There is an equilibrium at $r = \sum_{n=1}^{N} x^n$, so for $r < \sum_{n=1}^{N} (1/2)^n$, all trajectories starting on the attracting part of the manifold ($x < \frac{1}{2}$) will converge to an x-value of x^* that satisfies $r = \sum_{n=1}^{N} (x^*)^n$. For $r > \sum_{n=1}^{N} (1/2)^n$, trajectories starting on the attracting part of the manifold will move toward the fold point at $x = \frac{1}{2}$ and slip over it, moving away from the QSE where $x = 0$.

Ashwin et al. treat this as the tipping event with a critical rate at $r_c = \sum_{n=1}^{N}(1/2)^n$, where trajectories slip over the fold. But this doesn't quite represent the full story of this system. Numerical simulations show that for r slightly greater than r_c, trajectories will stay close to the fold point, cycling around the fold, instead of simply diverging away from the fold and the QSE (see Figure 2.2). It may be reasonable to consider this to be a form of tracking, with the state spiraling near the QSE.

2.2.2 Hopf Bifurcation in a Co-Moving System

To explain why the state begins tracking in a spiral, we will first reduce the system to an autonomous 2-dimensional system with a change of variables. Ashwin et al. call this a "co-moving" system, as the new variable increases along with the variable y and the rate parameter λ. In this system, we find a Hopf bifurcation with an emerging periodic orbit that corresponds to the spiraling trajectories. Set $v = y + \lambda$ and reduce the system (2.2) to one that is autonomous:

$$\begin{aligned} \epsilon\frac{dx}{dt} &= v + x(x-1) \\ \frac{dv}{dt} &= -\sum_{n=1}^{N} x^n + r. \end{aligned} \tag{2.6}$$

Theorem 10. *The co-moving system* (2.6) *has a Hopf bifurcation at* $r = \sum_{n=1}^{N}(1/2)^n$.

Proof. The equilibrium (x^*, v^*) for (2.6) is given by the solution to

$$\begin{aligned} \sum_{n=1}^{N}(x^*)^n &= r \\ v^* &= -x^{*2} + x^*. \end{aligned} \tag{2.7}$$

The Jacobian at this equilibrium is:

$$\begin{pmatrix} (2x^* - 1)/\epsilon & 1/\epsilon \\ \sum_{n=1}^{N} -n(x^*)^{n-1} & 0 \end{pmatrix}. \tag{2.8}$$

and the eigenvalues of the Jacobian are

$$\frac{2x^* - 1 \pm \sqrt{(1-2x^*)^2 - 4\epsilon\sum_{n=1}^{N} n(x^*)^{n-1}}}{2\epsilon}. \tag{2.9}$$

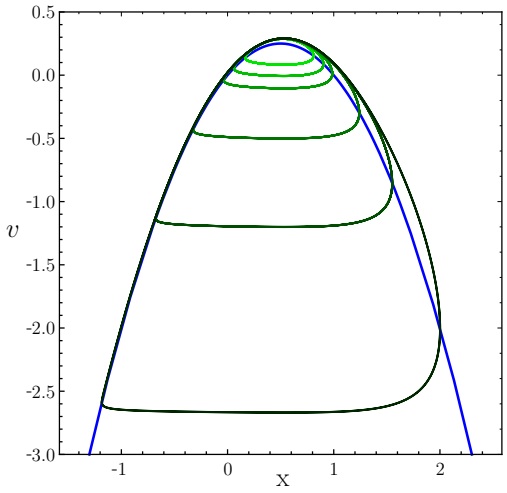

Figure 2.3: The parabolic critical manifold (blue) and several limit cycles in the co-moving system (2.6) where $\epsilon = .02$ for several values of $r > r_c = 0.9675$.

When $x^* < 1/2$, the equilibrium is asymptotically stable, which agrees with the conclusion in [2] that the system does not tip for $r < \sum_{n=1}^{N}(1/2)^n = r_c$. As r increases, so does x^*, so when $r = r_c$ and $x^* = 1/2$, the pair of eigenvalues are $\pm i\omega$ where

$$\omega = \sqrt{\sum_{n=1}^{N} n(1/2)^{n-1}/\epsilon}. \tag{2.10}$$

The eigenvalues cross the imaginary axis at $(x^*, w^*) = (1/2, 1/4)$, and when $x^* > 1/2$ (i.e. $r > r_c$), the equilibrium is unstable. To determine the type of Hopf bifurcation we calculate the first Lyapunov coefficient using the method of Chow, Li, and Wang [7]. The Jacobian at the bifurcation point, $x^* = 1/2$, is

$$J = \begin{pmatrix} a & b \\ c & d \end{pmatrix} = \begin{pmatrix} 0 & \frac{1}{\epsilon} \\ -\sum_{n=1}^{N} n(1/2)^{n-1} & 0 \end{pmatrix}. \tag{2.11}$$

Then the first Lyapunov coefficient (defined by Chow, Li, and Wang) is given by the

formula

$$\begin{aligned} l_1^{CLW} = \frac{b}{16\omega^4}\Big(& b(f_{xxx}+g_{vvv}) + 2d(f_{xxy}+g_{xvv}) - c(f_{xvv}+g_{xxv}) \\ & - bd(f_{xx}^2 - f_{xx}g_{xv} - f_{xv}g_{xx} - g_{xx}g_{vv} - 2g_{xv}^2) \\ & - cd(g_{vv}^2 - g_{vv}f_{xv} - g_{xv}f_{vv} - f_{vv}f_{xx} - 2f_{xv}^2) \\ & + b^2(f_{xx}g_{xx} - g_{xx}g_{xv}) - c^2(f_{vv}g_{vv} - f_{xv}f_{vv}) \\ & - (\omega^2 + 3d^2)(f_{xx}f_{xv} - g_{xv}g_{vv})\Big) \end{aligned} \tag{2.12}$$

where

$$\begin{aligned} f(x,v) &= (v + x(x-1))/\epsilon \\ g(x,v) &= -\sum_{n=1}^{N} x^n + r \end{aligned} \tag{2.13}$$

and each partial derivative in (2.12) is evaluated at $(x, v) = (1/2, 1/4)$. The only nonzero term in the sum is

$$\frac{b^3}{16\omega^4} f_{xx} g_{xx} \tag{2.14}$$

which evaluates to

$$l_1^{CLW} = -\Big(\frac{1}{16\epsilon^3\omega^4}\Big)\Big(\frac{2}{\epsilon}\Big)\Big(\frac{21}{2}\Big) < 0. \tag{2.15}$$

As l_1^{CLW} is negative, it implies that a supercritical Hopf bifurcation occurs at $r = r_c$, and a branch of stable periodic orbits bifurcates from $(1/2, 1/4)$ as r increases beyond r_c. □

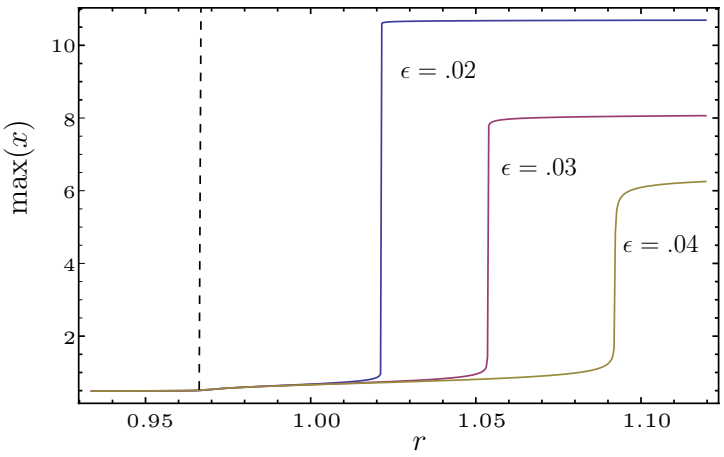

Figure 2.4: The numerically determined maximum distance of the the limit cycle from the QSE as a function of the rate, r, for $\epsilon = .02$, $\epsilon = .03$, and $\epsilon = .04$. The rate for which there is a Hopf bifurcation is $r = 0.96875$. The dotted line shows the limit curve as ϵ goes to 0.

As r increases beyond r_c, the size of this limit cycle grows continuously. It may be possible to prove analytically that there is a single attracting limit cycle for all $r > r_c$. That task could prove as challenging as a proof of the continuous progression of canard cycles in the van der Pol system. We show the progression of cycles numerically in Figure 2.4.

Corollary 11. *There is a positive neighborhood of the critical rate (i.e. $r \in (r_c, r_c + \delta)$ for some $\delta > 0$) for which trajectories follow spiraling curves $(x^*(t), w^*(t) - rt, rt)$, where $(x^*(t), w^*(t))$ is the asympototically stable limit cycle in the co-moving system* (2.6).

These numerical simulations show the system has an attracting limit cycle, which grows quickly for $r > r_c$. With the attracting periodic orbit growing continuously with r, naming a tipping point becomes an arbitrary designation. The Hopf bifurcation proves there are values of r greater than r_c such that an attracting solution cycles around the fold in a small periodic orbit. The value of r_c describes a bifurcation point, but an increase from close tracking to a large excursion is not immediate at the value r_c. The maximum distance of the state to the QSE is a continuous function of r even at r_c. We

show this maximum distance for several values of ϵ in Figure 2.3. It is only as ϵ tends to 0 that the size of the limit cycle grows infinite.

Not only is the maximum distance a continuous function of r, but it appears the greatest increase in maximum distance from the QSE occurs for a rate larger than the critical rate for trajectories surpassing the fold. In Figure 2.4 we can see the size of the limit cycle reaches a plateau. The reason for this is the relative strength of the quintic function $-\sum_{n=1}^{N} x^n$ with $N = 5$ compared to the quadratic isocline $w = x(1-x)$ where $\dot{x} = 0$. The limit cycle cannot grow too large in the positive x direction without being forced downward past $x(1-x)$ and turning back.

Some authors have analyzed a similar canard phenomenon as an equilibrium crosses a folded node. In one paper on aircraft ground dynamics [23], the canard cycles also have a plateauing behavior, but for a different reason. In that example, solutions are limited in their growth because the isocline $\dot{x} = 0$ has a second fold like a cubic function. In the next section we examine a similar system in which the return mechanism is due to a cubic isocline.

2.3 Forced van der Pol Oscillator

In this section, we analyze a linearly forced van der Pol oscillator to demonstrate the progression of spiraling trajectories similar to those of system (2.2). The van der Pol system has been well studied; we merely transform the equation slightly to demonstrate a rate-dependent bifurcation. The forced van der Pol oscillator as a second order ODE is given by

$$\frac{d^2x}{d\tau^2} - \mu(x^2-1)\frac{dx}{d\tau} + x = f(\tau). \tag{2.16}$$

We modify this by writing $f(\tau) = g(\tau) - \alpha$ to have

$$\frac{d^2x}{d\tau^2} - \mu(x^2-1)\frac{dx}{d\tau} + x = g(\tau) - \alpha \tag{2.17}$$

where α is a constant. Next, with the time transformation $t = -\tau/\mu$ we have

$$\frac{1}{\mu^2}\frac{d^2x}{dt^2} + (x^2-1)\frac{dx}{dt} + x = g(-\mu t) - \alpha. \tag{2.18}$$

Using the transformation

$$y = \frac{1}{\mu^2}\frac{dx}{dt} - (x - \frac{x^3}{3}) + \int_0^t g(-\mu s)ds, \tag{2.19}$$

and setting $\lambda(t) = \int_0^t g(-\mu s)ds$ and $\epsilon = \frac{1}{\mu^2} << 1$, we end up with a fast/slow system of equations:

$$\begin{aligned} \epsilon\frac{dx}{dt} &= y + (x - \frac{x^3}{3}) + \lambda(t) \\ \frac{dy}{dt} &= -x - \alpha. \end{aligned} \tag{2.20}$$

The van der Pol oscillator has been historically transformed so the forcing appears in the differential equation for the y variable [14, 30]. With the transformation into (2.20), the forcing $\lambda(t)$ is in the x equation as in the previous fast/slow system. As before, we assume λ changes linearly at a given rate r, so $\lambda(t) = rt$. This is equivalent to setting g to have a constant value of r.

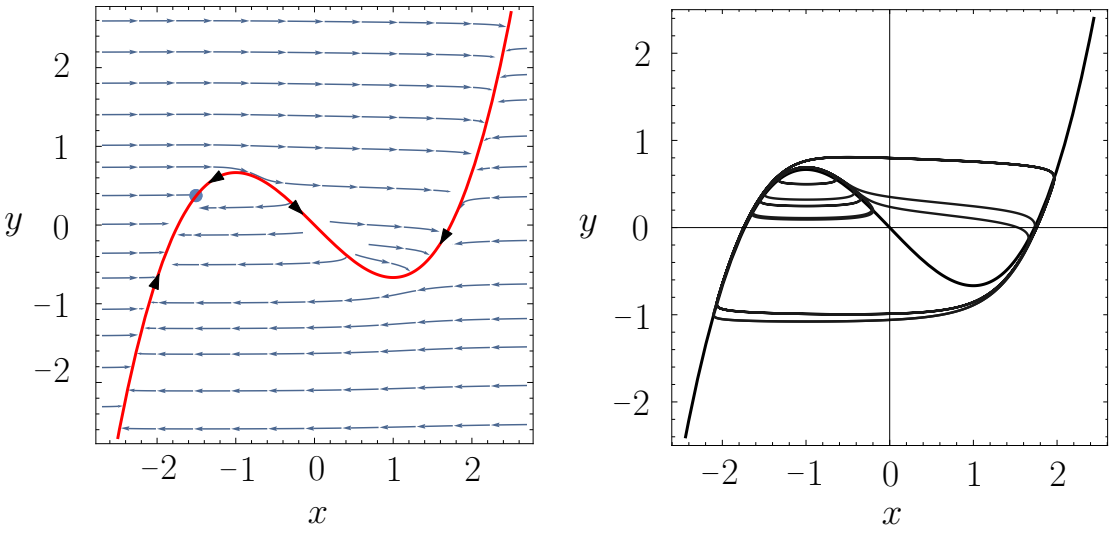

Figure 2.5: Left: phase portrait of the system in (2.20) for fixed $\lambda = 0$. The cubic slow manifold is in red, with the dot marking the stable equilibrium. Right: trajectories plotted for various values of r, illustrating the progression of the Hopf bifurcation and canard explosion in (2.21).

In equation (2.20), for a fixed constant $\alpha > 1$ and any fixed value of λ, this system has a stable equilibrium at $(x^*, y^*) = (-\alpha, -\alpha + \frac{\alpha^3}{3} - \lambda)$. A phase portrait with $\lambda = 0$ is shown in Figure 2.5. We create the co-moving system with the new variable, $w = y + \lambda$:

$$\begin{aligned} \epsilon \frac{dx}{dt} &= w + (x - \frac{x^3}{3}) \\ \frac{dw}{dt} &= -x - \alpha + r. \end{aligned} \tag{2.21}$$

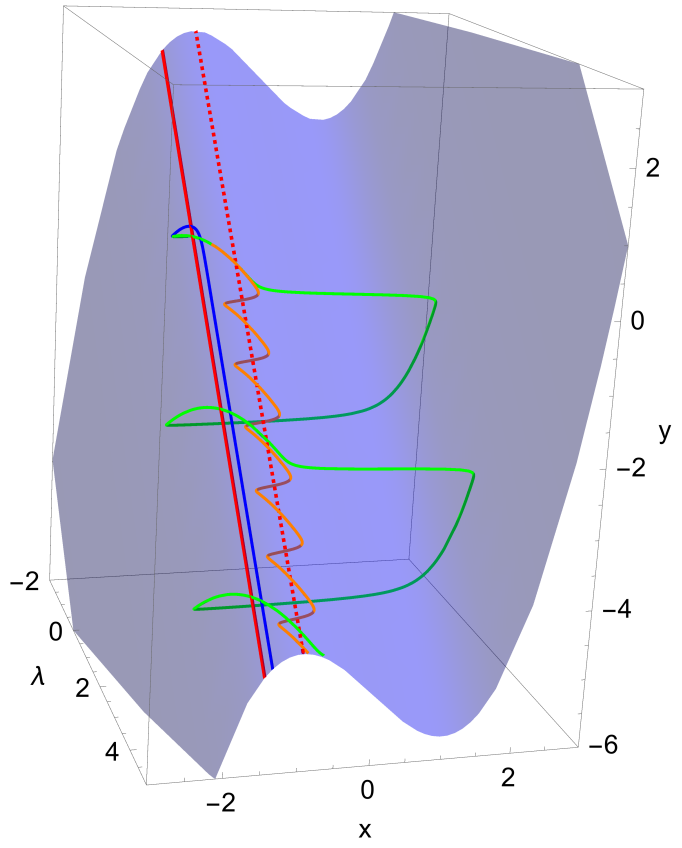

Figure 2.6: The slow critical manifold of the forced van der Pol system is shown; the solid red line shows the QSE and the dashed red line shows the fold. Three trajectories are plotted which exhibit three types of behavior: tracking the QSE closely ($r = 0.1$), tracking in a small spiral ($r = 0.5025$), and tracking as a large canard trajectory ($r = 0.503$).

This reduction results in a standard van der Pol system with r as the bifurcation parameter, as in [3] and [11]. In this system, a Hopf bifurcation occurs when $r = \alpha - 1$.

The periodic orbit formed at the Hopf bifurcation progresses quickly through a canard explosion (see Figure 2.5), with a rate-dependent tipping point at $r = \alpha - 1$. Like in the previous system, as the tipping occurs, the state spirals around the equilibrium. If the rate is high enough in (2.21), this spiral will be in the shape of the large canard trajectory. Due to the cubic isocline, for even higher rates, at $r > \alpha + 1$, the co-moving system again has a stable equilibrium on the other branch of the critical manifold. The state no longer spirals, but follows the QSE at a much further distance.

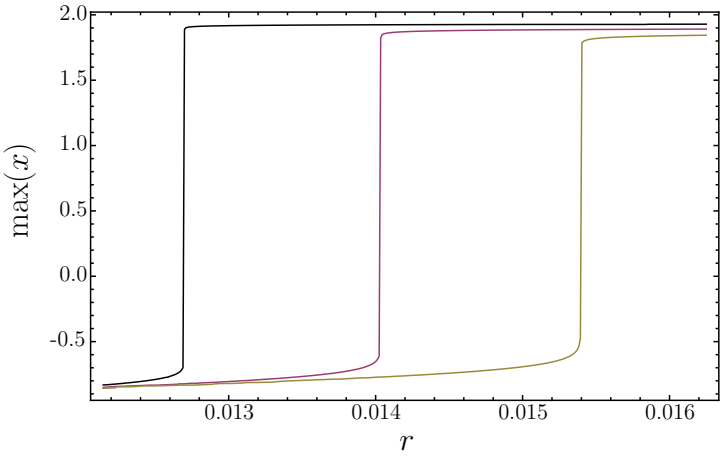

Figure 2.7: The canard explosion in the van der Pol System. The maximum distance of the limit cycle as r increases has been plotted for $\epsilon = .02$, $\epsilon = .03$, and $\epsilon = .04$. For this figure we set $\alpha = 1.01$, so the Hopf bifurcation occurs at $r = 0.01$.

The continuous progression of a single attracting limit cycle in the van der Pol system is well known, and has been confirmed by numerical simulation to show the continuous growth of the limit cycle as r increases. Once again, at the point where trajectories slip over the fold, they continue to track the QSE in a spiral. We postulate that this spiraling behavior occurs in this form of tipping over a fold in general. This example again raises the question of whether to consider this a "tipping point" as the maximum distance to the QSE still grows continuously.

2.4 Rosenzweig-MacArthur Model

The third model we examine comes from a paper on rate-dependent tipping points in ecological models by Siteur et al. [28]. It is a model of resource densities, R, and consumer densities, C:

$$\begin{aligned} \frac{dR}{dt} &= \lambda R\big(1 - \frac{R}{K}\big) - \frac{aCR}{R + R_h} \\ \frac{dC}{dt} &= \epsilon\big(\frac{eaCR}{R + R_h} - mC\big). \end{aligned} \tag{2.22}$$

Here λ is the resource growth rate, a parameter which declines steadily over time in our system to model a change in the ecosystem. Table 2.1 outlines the details of the rest of the parameters.

Parameter	Meaning	Unit	Value(s) Used
λ	resource growth rate	day^{-1}	$1 < \lambda < 5$
K	carrying capacity	g m^{-2}	10
a	max consumption rate	day^{-1}	1
R_h	value of R at which consumption is $a/2$	g m^{-2}	2
e	efficiency constant	unitless	1
m	consumer mortality rate	day^{-1}	0.7
ϵ	time scale parameter	unitless	0.1

Table 2.1: Parameters in the Rosenzweig-MacArthur Model and the values we use for simulation in this section.

In the first quadrant ($R, C > 0$), the isoclines of this system, shown in Figure 2.8, are given by the line

$$R = \frac{mR_h}{ea - m} \tag{2.23}$$

and the parabola

$$C = \frac{\lambda(k - R)(R + R_h)}{ak}. \tag{2.24}$$

The stable equilibrium (R^*, C^*) is the intersection of these isoclines at

$$\begin{aligned} R^* &= \frac{mR_h}{ea - m} \\ C^* &= \frac{\lambda}{ak}\left(k - \frac{mR_h}{ea - m}\right)\left(\frac{mR_h}{ea - m} + R_h\right). \end{aligned} \tag{2.25}$$

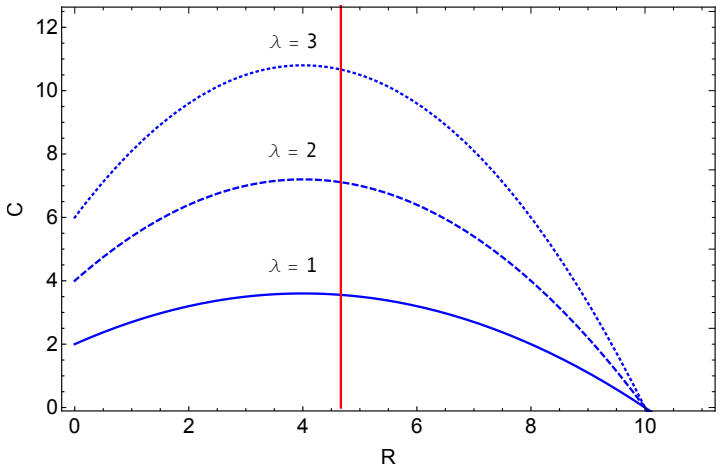

Figure 2.8: The isoclines of the system (2.22), plotted for three values of λ. The quadratic isocline $\frac{dC}{dt} = 0$ flattens as λ decreases.

The small parameter ϵ controls the difference in time scales, and in this fast/slow system the slow manifold is given by the quadratic isocline (2.24). As λ decreases, the quadratic isocline as well as the equilibrium shifts downward. This system differs from the last two in that the quadratic slow manifold also flattens as λ decreases, and λ cannot decrease indefinitely.

Yet, again, if we vary λ at a high enough rate, the solution tips over the fold of the critical manifold. Siteur et al. provide some analysis and numerical evidence of a critical rate at which the solution tips. However, the critical rate they find analytically depends on the value of λ, which of course is changing over time. This may account for the disparity in the values they find analytically and through numerical simulation.

Upon closer inspection of this system, we again find that for certain parameters and rates, the solutions spiral, rather than simply tip over the fold. We show some of these solutions in Figure 2.9. Unlike in the previous two examples, we cannot reduce

the system to one that is autonomous, so it is more difficult to analytically prove the existence of these spiraling solutions.

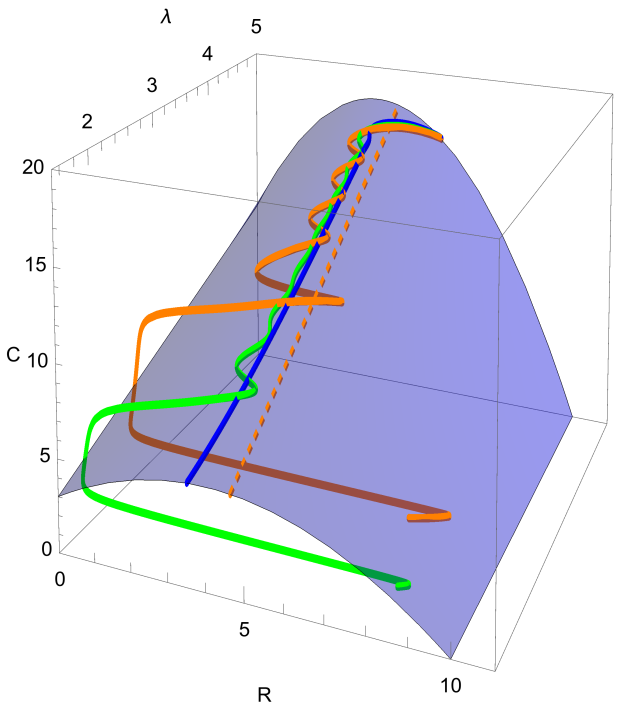

Figure 2.9: The surface shows the critical manifold in the system (2.22). The dashed line shows the QSE, and the other curves show trajectories for several rates of $\frac{d\lambda}{dt}$, with spiraling behavior for higher rates.

Situer et al. present some analysis of the lag of a solution to the QSE, which we expand upon. Again, we find something similar to a Hopf bifurcation, although the bifurcation point also depends on the changing value of λ.

Let $x = R - R^*$ and $y = C - C^*$ be variables that represent the lag between a solution to the system, $(R(t), C(t))$, and the moving QSE, $(R^*(t), C^*(t))$, given in equation (2.25). Then, calculating

$$\frac{dx}{dt} = \frac{dR}{dt} - \frac{dR^*}{d\lambda}\frac{d\lambda}{dt} \quad \text{and} \quad \frac{dy}{dt} = \frac{dC}{dt} - \frac{dC^*}{d\lambda}\frac{d\lambda}{dt}, \tag{2.26}$$

we have the following system of equations for the lag:

$$\begin{aligned}\frac{dx}{dt} &= \lambda(R^*+x)\big(1-\frac{R^*+x}{K}\big)-\frac{a(C^*+y)(R^*+x)}{R^*+x+R_h}\\ \frac{dy}{dt} &= \epsilon\big(\frac{ea(C^*+y)(R^*+x)}{R^*+x+R_h}-m(C^*+y)\big)-\Big(\frac{d\lambda}{dt}\Big)\frac{(k-R^*)(R^*+Rh)}{ak}.\end{aligned} \tag{2.27}$$

Note that λ (and therefore C^*) depends on time, so this system is nonautonomous. However, if we consider λ and C^* to be held constant, we can analyze the system as if it were autonomous, controlling the parameter $\frac{d\lambda}{dt}$. Doing so, we again find a Hopf bifurcation at a certain value of $\frac{d\lambda}{dt}$. If we use the same parameter values as Siteur et al., the bifurcation point is near the critical tipping rate they found numerically. We will analyze the system with the values in Table 2.1.

We continue our analysis with the numeric values in place of each parameter as well as setting $\lambda = 2$. This system, with the bifurcation parameter $\dot{\lambda} = \frac{d\lambda}{dt}$, is given by

$$\begin{aligned}\frac{dx}{dt} &= -\frac{(14+3x)(15y+x(4+3x))}{300+45x}\\ \frac{dy}{dt} &= \frac{(64+9y)x}{100(20+3x)}-\big(\frac{32}{9}\big)\dot{\lambda}.\end{aligned} \tag{2.28}$$

The lag system has an equilibrium at

$$(x^*,y^*) = \Big(\frac{8}{3}-\frac{8}{9}\sqrt{9-750\dot{\lambda}},\frac{32}{27}(-3+\sqrt{9-750\dot{\lambda}}+100\dot{\lambda})\Big). \tag{2.29}$$

The Jacobian at the equilibrium is given by

$$J(x^*,y^*) = \begin{pmatrix} a & b\\ c & d\end{pmatrix} = \begin{pmatrix} \frac{2}{15}-\frac{2x^*}{5}-\frac{2(64+9y^*)}{(20+3x^*)^2} & -1+\frac{6}{20+3x^*}\\ \frac{64+9y^*}{5(20+3x^*)^2} & \frac{9x^*}{2000+300x^*}\end{pmatrix}. \tag{2.30}$$

The real and imaginary parts of the eigenvalues are plotted in Figure 2.10. The equilibrium is unstable for $\dot{\lambda} < -.006894$. At the bifurcation point the eigenvalues $E_\pm(\dot{\lambda})$ equal $\pm i\omega$, where $\omega = 0.1635$.

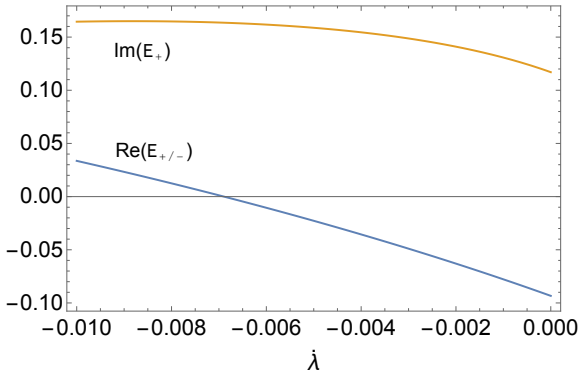

Figure 2.10: The upper curve shows the positive imaginary part of the eigenvalues, $\mathrm{Im}(E_+(\dot{\lambda}))$; the lower curve shows the real part of the eigenvalues, $\mathrm{Re}(E_\pm(\dot{\lambda}))$. At $\dot{\lambda} = -.006894$ we see the transition from a stable to unstable equilibrium as $\dot{\lambda}$ decreases.

Again, we can calculate the first Lyapunov coefficient using equation 2.12. For these parameters we find $l_1^{CLW} = -0.129 < 0$. This implies that a supercritical Hopf bifurcation occurs, and a curve of stable limit cycles exists for a range of values of $\dot{\lambda}$ below the bifurcation value.

This bifurcation analysis can repeated for any fixed value of λ. As mentioned before, the system is not reducible to an autonomous one, so the analysis of a Hopf bifurcation is less reliable, but it still gives us insight into the behavior of the nonautonomous system. In general, when the rate of $\dot{\lambda}$ is more negative, we find the spiraling instability occurs sooner, but the divide between steady tracking and spiraling is not quite as well-defined as in the previous examples.

2.5 Bifurcations in Nonautonomous Systems

The fast/slow nonautonomous systems in the first two examples are reducible into autonomous systems with a simple coordinate change because the forcing function λ has a constant derivative and the vector fields simply shift as λ changes. In autonomous systems, we can more easily determine the progression of stationary equilibrium points and limit cycles; in particular, index theory of isolated invariant sets can tell us a lot about how invariant sets may change with respect to a parameter. In this example, it

would be possible to find an isolating neighborhood of the equilibrium for a range of the parameter around the critical value. The index associated to this neighborhood would have to remain the same for all values of the parameter in this range. Since the index of a stable equilibrium differs from an unstable equilibrium, we could deduce that as the parameter crosses the critical value, there must be another invariant set (the limit cycle) inside this neighborhood. This contrasts with our original notion of rate-dependent tipping: the idea that trajectories stop tracking once a critical threshold is reached.

If we only consider the original nonautonomous system in the coordinate space (x, y, t), our simulations indicate that an attracting steady line bifurcates into an attracting spiral as the rate parameter increases. We were able to prove that this happens in the first two examples because we could reduce the system to an autonomous one which had a Hopf bifurcation. This observation motivates the following general question: how would we go about analyzing this phenomenon in a nonautonomous system for which there exists no such reduction into an autonomous system, as is the case in the Rosenzweig-MacArthur model? One method, which we will begin to develop in the next few chapters, would be to find nonautonomous isolating blocks, where the behavior of the system on the boundary of the blocks can tell us about the invariant sets inside. Using these blocks, we will see that the spiraling invariant sets we discovered in this chapter are robust under nonautonomous perturbations; that is, the structure of the solutions will persist even when the forcing function is $\lambda = rt + \epsilon(t)$, for a nonautonomous perturbation $\epsilon(t)$.

Chapter 3

Isolating Blocks for Nonautonomous Flows

A great deal of work has been done in classifying invariant sets of autonomous flows. In the late 1940s, Ważewski wrote several papers on the existence of invariant sets in autonomous systems, given knowledge of the flow on the boundary of some region. Beginning in 1969, Easton and Conley expanded on this, analyzing the existence of invariant sets inside a "manifold convex to a flow." The term "isolating block" was coined later to describe these compact sets. Easton included a characterization of the invariant sets based on the homology of the manifold [12]. This characterization was expanded in Conley's influential monograph [9] proving the existence of both an index of an isolated invariant set and the Morse decomposition of invariant sets. The index, based on the homotopy type of the isolating block, is known as the Conley index, and for isolated equilibrium points in an autonomous system, it coincides with the Morse index.

We are interested in invariant sets for many reasons. Attracting invariant sets can tell us how solutions will behave as time progresses. For certain situations, such as an orbiting satellite, it may be desirable to keep an object near a "saddle" or repelling invariant solution. Although nearby trajectories will not approach a repelling solution, they will not move away too quickly either. Like balancing an upright rod on your finger, it takes only a small amount of energy to correct the state of an object in the

system, moving it back toward the repelling invariant solution.

Many physical systems are nonautonomous, and it is not as obvious what we mean by an invariant set in such a system, where forces and trajectories might depend on time. In this chapter, by "invariant set" we mean a collection of solutions which stay inside a region in $\mathbb{R} \times X$ that we prescribe. We propose a definition of isolating blocks for (continuous-time) nonautonomous flows and (discrete) nonautonomous maps, and prove the existence of invariant sets under certain conditions on these isolating blocks. Ideally, we would like an index to classify nonautonomous invariant sets, but difficulties arise when attempting to devise a well-defined Conley index in a space that is not compact.

Recently a Conley index was formulated for nonautonomous skew-product semiflows [16]. In this formulation, flows must satisfy an "admissibility" requirement, which is a substitute for the compactness requirement in autonomous flows. Nonautonomous flows, in general, do not satisfy such a requirement unless there is a periodicity or another similar aspect to its time-dependence. Within the last decade, Conley's theory has also been extended by Liu to random dynamical systems [18]. This setting is very similar to nonautonomous systems, if the random variable is swapped for a time-varying parameter. We will make use of some techniques from Liu's work on random dynamical systems, as well as Franks and Richeson's work on a Conley index for maps [13], in order to prove statements about isolated invariant sets of nonautonomous maps.

For nonautonomous maps, we prove that isolating blocks of invariant sets persist under perturbation. In Chapter 4, we will show this is true for certain isolating blocks in nonautomous flows. This further proves that invariant sets persist in perturbations of nonautonomous systems, and notably, in examples of rate-dependent bifurcations like the ones in the previous chapter. We also prove a statement (similar to Ważewski's Theorem) concerning the existence of invariant solutions for nonautonomous flows where the isolating block appears constant in some moving frame of reference.

3.1 Nonautonomous Flows and Maps

Let X be a locally compact metric space, with metric d_X. We say that $\phi : \mathbb{R}\times\mathbb{R}\times X \to X$ is a *nonautonomous flow* on X if $\phi(t, s) \coloneqq \phi(t, s, \cdot) : X \to X$ is a continuous map for

all $t, s \in \mathbb{R}$, and

$$\begin{aligned} \phi(0, s) &= \mathrm{id}_X \\ \phi(t + r, s) &= \phi(t, r + s) \circ \phi(r, s). \end{aligned} \tag{3.1}$$

Some authors call ϕ a *process* or a *nonautonomous dynamical system* (for example, [4, 5, 6, 24]) but we will use the term *nonautonomous flow* as it harkens more toward the theories of Conley and Ważewski.

Given a nonautonomous flow ϕ, we can make a true flow on $\mathbb{R} \times X$ by including time as a state variable as in equation (1.9), defining $\Phi : \mathbb{R} \times \mathbb{R} \times X \to \mathbb{R} \times X$ by

$$\Phi(t, s, x) = (t + s, \phi(t, s)x). \tag{3.2}$$

We will call Φ the *time-extended flow* of ϕ. In equation (3.2) we should think of s as the starting time of the flow, and t as the elapsed time. Then $\phi(t, s)x$ gives the new state at time $t + s$.

Each map $\phi(t, s) : X \to X$ is a homeomorphism with inverse $\phi(-t, s)$. We can restrict t and s to the integers to form a *discrete nonautonomous flow* $\phi : \mathbb{Z} \times \mathbb{Z} \times X \to X$. In section 3.2, we will consider discrete nonautonomous flows rather than continuous-time nonautonomous flows. To simplify notation, we write $\varphi(k) = \phi(1, k) : X \to X$ to be the time-one map of ϕ at time k. We will call φ a *nonautonomous map*. We also use the notation $\varphi^m(k) \coloneqq \phi(m, k) = \varphi(k + m - 1) \circ ... \circ \varphi(k + 1) \circ \varphi(k)$. With this notational system, although it may not be ideal, we must accept that $\varphi^{-1}(k + 1)$ is equal to $(\varphi(k))^{-1}$ (see Figure 3.1).

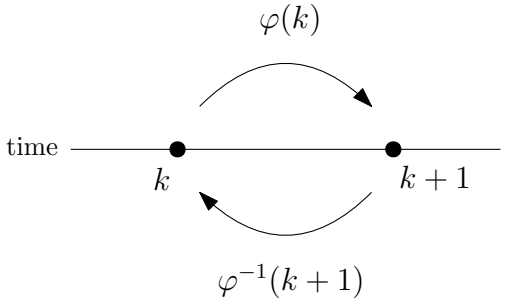

Figure 3.1: $\varphi(k)$ sends points at time k to points at time $k+1$, while $\varphi^{-1}(k+1)$ sends points at time $k + 1$ to points at time k.

3.2 Isolated Invariant Sets of Nonautonomous Maps

In this section, we will call A a nonautonomous set when $A(k)$ is a subset of X for all $k \in \mathbb{Z}$. We say A is compact if $A(k)$ is compact for all k, and $A \subset B$ if $A(k) \subset B(k)$ for all k.

Definition 12. A nonautonomous set D is *forward invariant* if $\varphi^n(k)D(k) \subset D(k+n)$, for all $k \in \mathbb{Z}$, $n \in \mathbb{Z}^+$. D is *backward invariant* if $\varphi^n(k)D(k) \supset D(k+n)$ for all $k \in \mathbb{Z}$, $n \in \mathbb{Z}^+$. And D is *invariant* if $\varphi^n(k)D(k) = D(k+n)$ for all $n, k \in \mathbb{Z}$.

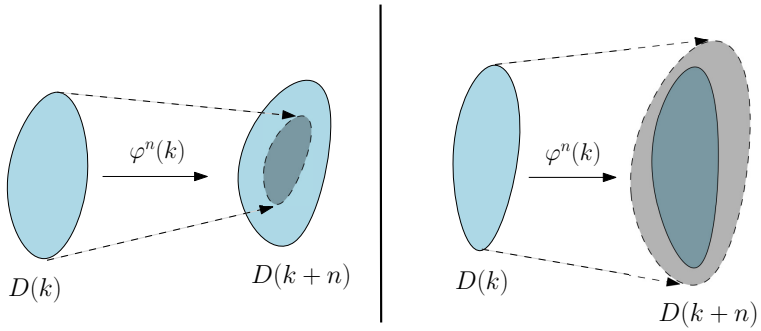

Figure 3.2: Left: An illustration of forward invariance. Right: Backward invariance.

Definition 13. Let N be a nonautonomous set in X. The invariant set of N is defined as

$$\mathrm{Inv}(N, \phi)(k) \coloneqq \{x \in N(k) \mid \phi(n,k)x \in N(k+n) \text{ for all } n \in \mathbb{Z}\}. \tag{3.3}$$

Definition 14. A compact nonautonomous set N is called a *nonautonomous isolating neighborhood* if it satisfies $\mathrm{Inv}(N, \phi)(k) \subset \mathrm{int}\ N(k)$ for all $k \in \mathbb{Z}$.

Definition 15. A nonautonomous set S is called an *isolated invariant set* if there exists a nonautonomous isolating neighborhood N such that $S(k) = \mathrm{Inv}(N, \phi)(k)$ for all $k \in \mathbb{Z}$.

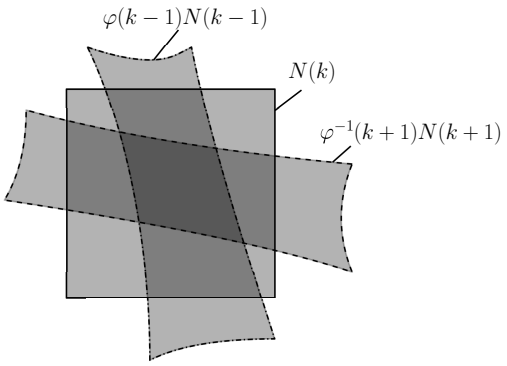

Figure 3.3: An isolating block for a nonautonomous map. The intersection of the three sets shown lies in the interior of $N(k)$.

Definition 16. A compact nonautonomous set N is called a *nonautonomous isolating block* if

$$\varphi(k-1)N(k-1) \cap N(k) \cap \varphi^{-1}(k+1)N(k+1) \subset \text{int } N(k) \text{ for all } k \in \mathbb{Z}. \tag{3.4}$$

Figure 3.3 demonstrates condition (3.4). As in the autonomous case, a nonautonomous isolating block is an isolating neighborhood, but the converse is not necessarily true.

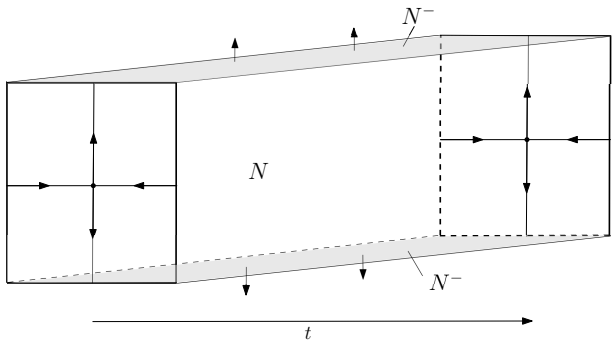

Figure 3.4: A nonautonomous saddle equilibrium and the exit set N^- on the boundary of a nonautonomous isolating neighborhood N.

Definition 17. Given a nonautonomous isolating neighborhood N, the exit set N^- of N is defined as

$$N^-(k) \coloneqq \{x \in N(k) \mid \varphi(k)x \notin \text{int } N(k+1)\}. \tag{3.5}$$

Isolating blocks have the property that every point on the boundary of $N(k)$ is in the exit set for either $\varphi(k)$ or for $\varphi^{-1}(k)$.

3.2.1 Isolating Blocks of Nonautonomous Maps

This section is devoted to proving the existence of isolating blocks of isolated invariant sets in nonautonomous maps. Franks and Richeson give a method based on ϵ-chains to construct isolating blocks for autonomous systems [13]. Unfortunately, this method does not work for us, mainly because $\mathbb{Z} \times X$ is not compact.

We can still prove the existence of isolating blocks in discrete nonautonomous systems, but this is partially due to the great amount of freedom we have in choosing the set for each time k. Our proof constructs isolating blocks that are somewhat degenerate because they may contract around the invariant set; however, we include it because its existence shows that invariant sets are persistent under certain perturbations.

Theorem 18. *Given a nonautonomous isolated invariant set S with a compact nonautonomous isolating neighborhood N for the nonautonomous map φ, there exists a nonautonomous isolating block of S.*

Proof. For each $k \in \mathbb{Z}$, since $S(k) \subset \text{int } N(k)$, and $S(k)$ is compact, there exists a compact neighborhood B_k of $S(k)$ such that $B_k \in \text{int } N(k)$. Set $B(0) = B_0$. Since $S(0) \subset \text{int } B(0)$, and $S(0)$ is compact, we can find a compact neighborhood B_0^* of $S(0)$ such that $B_0^* \in \text{int } B(0)$. Then $\varphi(1)B_0^* \cap B_1$ must be a compact neighborhood of $S(1)$. Set $B(1) = \varphi(0)B_0^* \cap B_1$.

In the same manner, for each $k \in \mathbb{N}$, find a compact neighborhood B_k^* of $S(k)$ such that $B_k^* \subset \text{int } B(k)$, and set $B(k+1) = \varphi(k)B_k^* \cap B_k$. Then, by construction, since $B_k^* \in \text{int } B(k)$, we have

$$\varphi^{-1}(k+1)B(k+1) \subset \text{int } B(k), \tag{3.6}$$

so for $k \geq 0$, $B(k)$ satisfies the condition to be an isolating neighborhood.

Likewise, set $B(-1) = \varphi^{-1}(0)B_0^* \cap B_{-1}$, and for each $k < 0$, find a compact neighborhood B_k^* of $S(k)$ with $B_k^* \subset \text{int } B(k)$, and set $B(k-1) = \varphi^{-1}(k)B_k^* \cap B_{k-1}$. Since $\varphi^{-1}(k)$ is a homeomorphism, this will also be a compact neighborhood of $S(k-1)$, and

in this case, for $k \leq 0$ we have

$$\varphi(k-1)B(k-1) \subset \text{int } B(k), \tag{3.7}$$

so $B(k)$ also satisfies the condition of being an isolating block for $k \leq 0$. Thus, the compact nonautonomous set B is an isolating block. □

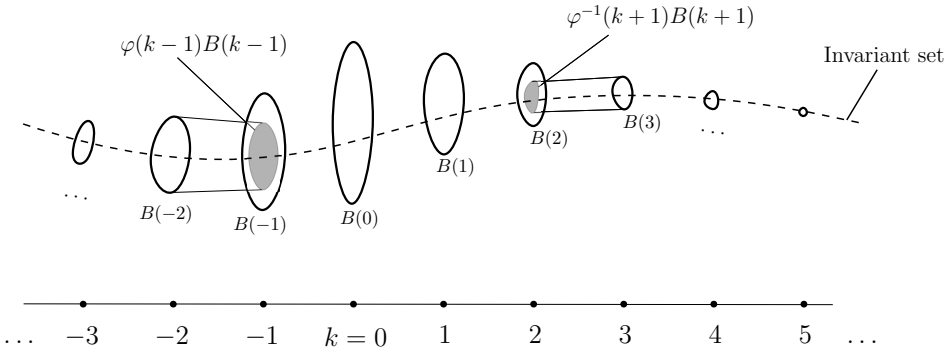

Figure 3.5: An isolating block which expands around the invariant set for $k < 0$ and contracts for $k > 0$.

There are drawbacks to this construction of an isolating block. For $k < 0$, since we have $\varphi(k-1)B(k-1) \subset \text{int } B(k)$, it appears that the invariant set inside is an attractor. However, for $k > 0$, we have $\varphi^{-1}(k+1)B(k+1) \subset \text{int } B(k)$, and it appears that the invariant set inside is a repelling invariant set. This is simply because we chose $B(k)$ to expand around $S(k)$ for $k < 0$, and we chose it to contract for $k > 0$ (see Figure 3.5).

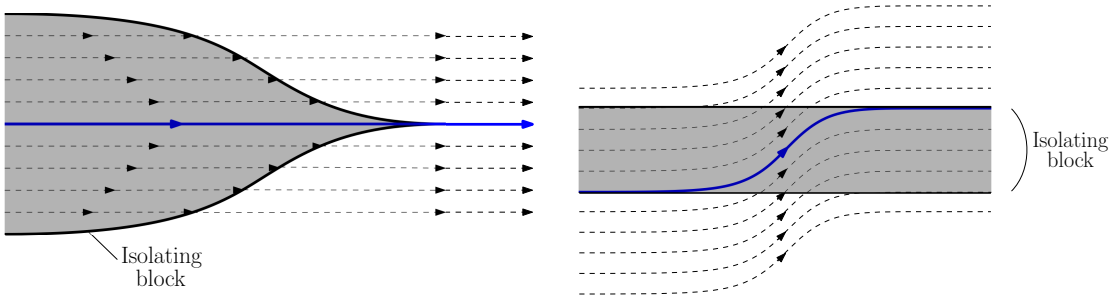

Figure 3.6: Left: An invariant set (solid line) in a constant flow which is only "isolated" because the isolating neighborhood (shaded) contracts around it. Right: An isolated invariant set (solid line) with a constant isolating block (shaded) that it approaches asymptotically.

Stronger Conditions on an Isolating Block

Our loose definition of an isolating block also allows for the existence of isolated invariant sets which approach the boundary of the block asymptotically as time goes to positive or negative infinity, as shown in Figure 3.6. Given the possibility for these degenerate isolated invariant sets, it may be more practical to impose stronger restrictions on our definition of isolating block. For example, we may restrict how an invariant set approaches an isolating neighborhood. One could require an isolating block to remain a minimum distance from the invariant set. We define the minimum distance between sets $A, B \subset X$ as

$$\operatorname{dist}_X(A, B) \coloneqq \inf_{a \in A} \inf_{b \in B} d_X(a, b). \tag{3.8}$$

Restricting the isolating block to keep a minimum distance from the invariant set would be given then, by the condition

$$\inf_{k \in \mathbb{Z}} \operatorname{dist}_X(\operatorname{int}^c B(k), S(k)) > 0. \tag{3.9}$$

The construction in Theorem 18 would violate this as the isolating block may contract around the invariant set within arbitrarily small distances.

Alternatively, we could require some consistency in the structure of the isolating block and its exit set. For example, we could require the existence of a nonautonomous

map $\xi : \mathbb{Z} \times X \to X$ such that

$$\xi(k)B(k) = B(k+1) \quad \text{and} \quad \xi(k)B^-(k) = B^-(k+1). \tag{3.10}$$

These two conditions are depicted in Figure 3.7. Another property that would rule out the flow depicted in Figure 3.8 would be that any forward (or backwards) invariant trajectory $x(k)$ in B must approach an invariant set $S(k)$ in forward time, in that

$$\limsup_{k\to\infty} \operatorname{dist}_X(x(k), S(k)) = 0. \tag{3.11}$$

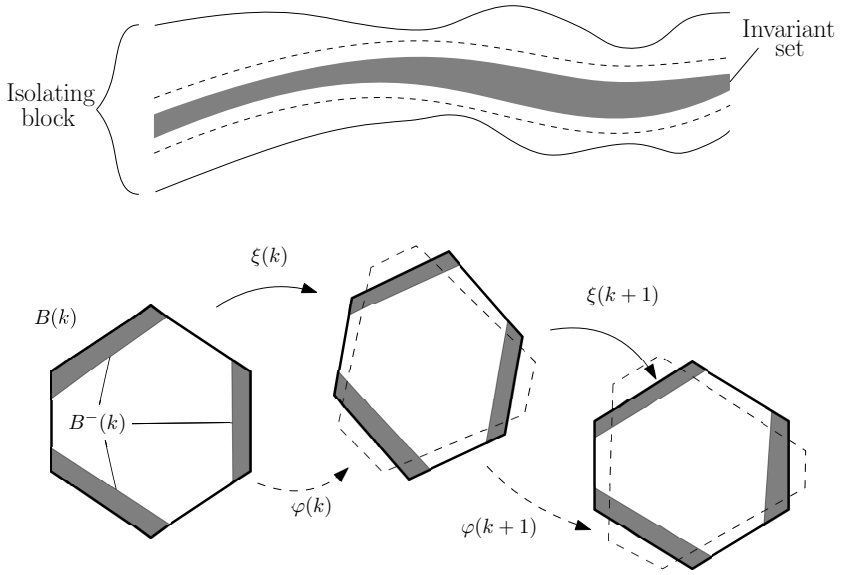

Figure 3.7: Top: an isolating block (in a continuous system) which remains a finite distance from the invariant set. Bottom: the isolating block $B(k)$ and its exit set $B^-(k)$ is transformed by the homeomorphism $\xi(k)$ at each time k. Dashed outlines show possible transformations by the nonautonomous map φ.

All three of these conditions are satisfied by isolating blocks for autonomous maps. In the following text we do not impose any of the conditions mentioned for nonautonomous isolating blocks, but in practice it may be wise to keep in mind when an isolating block violates one of these conditions. The downside to these restrictions is that even if they hold true for a nonautonomous map φ, they may not hold true for perturbations of φ.

In the next section, we address the stability of isolating blocks under perturbations of a nonautonomous flow.

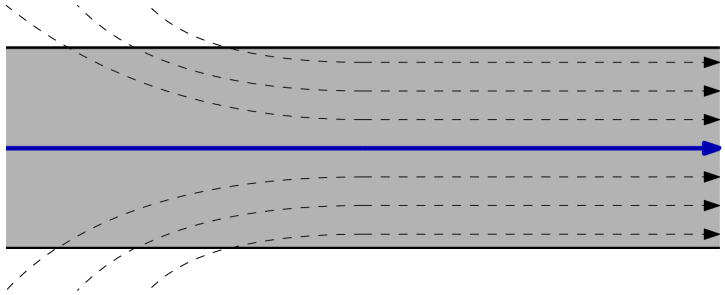

Figure 3.8: A flow where the forward invariant curves in the isolating block (shaded) do not asymptotically approach the invariant set.

3.2.2 Continuation of Isolating Blocks of Nonautonomous Maps

For autonomous flows, one main feature of isolating blocks is that they remain isolating blocks under small perturbations of the flow. To quantify a perturbation in a nonautonomous flow, we introduce a time-dependent metric.

Let φ, ψ be nonautonomous maps and N be a nonautonomous compact set. Define the function

$$\begin{aligned} d_N^k(\varphi,\psi) \coloneqq & \sup_{x\in N(k-1)} d_X(\varphi(k-1)x, \psi(k-1)x) \\ & + \sup_{y\in N(k+1)} d_X(\varphi^{-1}(k+1)y, \psi^{-1}(k+1)y). \end{aligned} \tag{3.12}$$

Then $d_N^k(\cdot,\cdot)$ is a time-dependent metric, in the sense that for each k, $d_N^k(\cdot,\cdot)$ is a metric on the space of continuous nonautonomous maps whose domain contains N, which we will denote $\mathcal{M}(N)$. Indeed, it is straightforward to check that

1. $d_N^k(\varphi,\psi) \geq 0$
2. $d_N^k(\varphi,\psi) = d_N^k(\psi,\varphi)$
3. $d_N^k(\varphi,\psi) = 0$ implies $\varphi(k)x = \psi(k)x$ and $\varphi^{-1}(k)x = \psi^{-1}(k)x$ for all $x \in N(k)$ and

4. $d_N^k(\psi_1, \psi_2) + d_N^k(\psi_2, \psi_3) \geq d_N^k(\psi_1, \psi_3)$.

Definition 19. We say $\mathcal{N}$ is a neighborhood of φ if there exists a function $\rho : \mathbb{Z} \to \mathbb{R}^+$ such that $B_\rho(\varphi) \subset \mathcal{N}$ where

$$B_\rho(\varphi) \coloneqq \{f \in \mathcal{M}(N) \mid d_N^k(f, \varphi) < \rho(k) \text{ for all } k \in \mathbb{Z}\} \tag{3.13}$$

For an autonomous map, f, Franks and Richeson [13] deliver a simple proof that if

$$f(N) \cap N \cap f^{-1}(N) \subset \text{int } N, \tag{3.14}$$

then this property (3.14) holds for functions in some neighborhood of f [13]. We use a similar argument to show that a corresponding property for nonautonomous isolating blocks holds true in a neighborhood of a nonautonomous map.

Theorem 20. *Suppose that N is a nonautonomous isolating block for $\varphi \in \mathcal{M}(N)$. Then there exists a nonautonomous neighborhood $\mathcal{N}$ of φ such that N is an isolating block for all $\psi \in \mathcal{N}$.*

Proof #1. Suppose that there is no neighborhood. Then there exists a sequence of nonautonomous maps $\{\psi_n\}$ converging to φ and a sequence of points $\{x_n\}$ such that

$$x_n \in \psi_n(k-1)N(k-1) \cap N(k) \cap \psi_n^{-1}N(k+1) \cap \text{int}^c N(k). \tag{3.15}$$

Then we may choose a subsequence $\{x_{n_j}\}$ which converges to a point $x^* \in \varphi(k-1)N(k-1)\cap N(k)\cap\varphi^{-1}N(k+1)\cap\text{int}^c N(k)$, which would contradict the fact that N is an isolating block for φ. □

Although this proof may be concise, it does not provide a value for the amount we may perturb φ while retaining the isolating block N. A slightly different line of reasoning gives a method to construct such a lower bound on perturbations of φ.

Proof #2. Fix $k \in \mathbb{Z}$. Define the sets $\tilde{N}$ and $\hat{N}$ by

$$\begin{aligned} \tilde{N} &= \varphi(k-1)N(k-1) \cap N(k) \cap \varphi^{-1}(k+1)N(k+1) \text{ and} \\ \hat{N} &= \varphi(k-1)N(k-1) \cap \text{int}^c N(k) \cap \varphi^{-1}(k+1)N(k+1). \end{aligned} \tag{3.16}$$

Since $\tilde{N} \subset \text{int } N(k)$, we may choose an open neighborhood W such that $\tilde{N} \subset \text{cl}(W) \subset \text{int } N(k)$. Let $\rho_1 = \text{dist}_X(\text{cl}(W), \text{int}^c N(k))$. Then since both of these sets are closed and disjoint, $\rho_1 > 0$.

We also have $\hat{N} \subset N^c(k)$, and since $N^c(k)$ is an open set, we must be able to find an open neighborhood V such that $\hat{N} \subset V^c \subset N^c(k)$. Let $\rho_2 = \text{dist}_X(V^c, N(k))$. Again, since both of these sets are closed and disjoint, $\rho_2 > 0$.

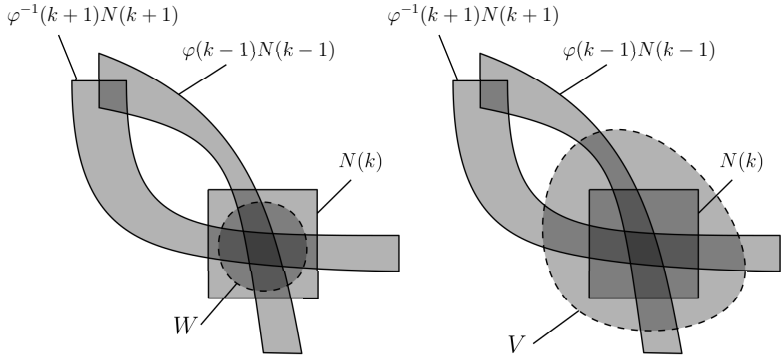

Figure 3.9: An illustration of the sets W and V defined in Proof #2.

Let $A = \varphi(k-1)N(k-1) \cap \text{cl}(V \setminus W)$ and $B = \varphi^{-1}(k+1)N(k+1) \cap \text{cl}(V \setminus W)$. Let $\rho_3 = \text{dist}_X(A, B)$. By our choice of V and W, A and B must be closed and disjoint, so $\rho_3 > 0$. Finally, find a value $\rho(k)$ such that

$$0 < \rho(k) < \min(\rho_1, \rho_2, \rho_3/2). \tag{3.17}$$

We will show that if $d_N^k(\psi, \varphi) < \rho(k)$, then $\psi(k-1)N(k-1) \cap N(k) \cap \psi^{-1}(k+1)N(k+1) \subset \text{int } N(k)$. Let $x \in N(k-1)$. Since $W \subset V$, $\varphi(k-1)x$ must be either in V^c, W, or $V \setminus W$.

Case 1: If $\varphi(k-1)x \in V^c$, then since $\rho < \text{dist}_X(V^c, N(k))$ and $d_X(\varphi(k-1)x, \psi(k-1)x) \leq \rho$, we have $\psi(k-1)x \notin N(k)$.

Case 2: If $\varphi(k-1)x \in W$, then since $\rho < \text{dist}_X(W, \text{int}^c N(k))$ and $d_X(\varphi(k-1)x, \psi(k-1)x) \leq \rho$, we have $\psi(k-1)x \notin \text{int}^c N(k)$.

Case 3: If $\varphi(k-1)x \in (V \setminus W)$, then $\varphi(k-1)x \in A$. If $\psi(k-1)x \cup N(k) \cup \psi^{-1}(k+1)N(k+1) \neq \emptyset$, there must exist $y \in N(k+1)$ such that $\psi^{-1}(k+1)y = \psi(k-1)x$. If

$\varphi^{-1}(k+1)y \in (V \setminus W)$, then $\varphi^{-1}(k+1)y \in B$. In this case,

$$\begin{aligned} d_X(\varphi^{-1}(k+1)y, \varphi(k-1)x) &\leq d_X(\varphi^{-1}(k+1)y, \psi^{-1}(k+1)y) + d_X(\psi(k-1)x, \varphi(k-1)x) \\ &< \rho_3/2 + \rho_3/2 = \rho_3. \end{aligned} \tag{3.18}$$

However, since $\varphi^{-1}(k+1)y \in B$ and $\varphi(k-1)x \in A$, the inequality in (3.18) would contradict the fact that $\text{dist}_X(A, B) = \rho_3$. Thus, $\varphi^{-1}(k+1)y$ is either in V^c or W. If $\varphi^{-1}(k+1)y \in V^c$, then by the same reasoning as in Case 1, $\psi^{-1}(k+1)y \notin N(k)$, and therefore $\psi(k-1)x \notin N(k)$. If $\varphi^{-1}(k+1)y \in W$, by the same reasoning as Case 2, $\psi^{-1}(k+1)y \notin \text{int}^c N(k)$, and $\psi(k-1)x \notin \text{int}^c N(k)$.

Thus, in all three cases, $\psi(k-1)x \cap N(k) \cap \psi^{-1}(k+1)N(k+1) \subset \text{int } N(k)$. Finding $\rho(k)$ for all integers k gives a function such that N is an isolating block for any $\psi \in B_\rho(\varphi)$. $\square$

Theorem 20 proves that invariant sets have some stability under nonautonomous perturbations. Used along with Theorem 18, it shows that for any system with an isolated invariant set, there exists a nonautonomous neighborhood of that system which has an isolated invariant set in the same isolating block. Due to the nature of the construction of isolating blocks in Theorem 18, it may be that this perturbation $\rho(k)$ has $\lim_{k\to\infty} \rho(k) = 0$ or $\lim_{k\to-\infty} \rho(k) = 0$. For nonautonomous perturbations of autonomous systems, though, the construction in Proof #2 above shows that $\rho(k)$ may be chosen to be constant, so that $\rho(k) > \epsilon$ for all k, for some value $\epsilon > 0$.

3.3 Comparing Nonautonomous Maps and Flows

Many applied systems that we wish to study are best represented by nonautonomous differential equations rather than nonautonomous maps. Solutions to nonautonomous differential equations are not a discrete sequence of points but a continuous function.

We proved the existence of isolating blocks of invariant sets only in the discrete case, and even then we only found degenerate isolating blocks. The existence of isolating blocks for continuous nonautonomous flows seems to be more difficult to prove. Yet, for most continuous flows, we can find a unit of time h that is small enough such that the invariant set of $\phi(t, s)$ within the continuous nonautonmous set $N(t)$ is the same as the invariant set of the nonautonomous map $\varphi : \mathbb{Z} \times X \to X$ given by the discretized flow $\varphi(k) = \phi(h, hk)$ for the discrete nonautomous set $\tilde{N}(k) = N(hk)$.

We began by analyzing discrete nonautonomous maps rather than continuous-time nonautonomous flows because the nonautonomous isolating blocks are easier to work with and structurally stable. To prove that the invariant sets of continuous-time systems are stable under perturbations, we can discretize time and show that the discrete isolating blocks are stable under discrete perturbations. As long as the continuous perturbations remain under some threshold when the system is discretized, the discrete isolating blocks remain. In certain cases it can be proven that a discrete isolating block must have a non-empty invariant set. Unfortunately, proving the existence of invariant sets for maps is less straightforward than for continuous systems. Ważewski's Theorem, for example, cannot be applied. We will continue this chapter by exploring alternative methods of finding invariant sets and isolating blocks in continuous-time nonautonomous flows.

3.4 Isolating Blocks of Nonautonomous Flows

The definition of isolated invariant sets within a continuous-time nonautonomous flow is nearly identical to the definition in the discrete case.

Definition 21. An isolating neighborhood in a nonautonomous flow ϕ is a compact nonautonomous set N such that $\mathrm{Inv}(N,\phi)(t) \subset \mathrm{int}\ N(t)$ for all $t \in \mathbb{R}$, where

$$\mathrm{Inv}(N,\phi)(t) \coloneqq \{x \in N(t) \mid \phi(s,t)x \in N(t+s) \text{ for all } s \in \mathbb{R}\}. \tag{3.19}$$

Then a nonautonomous isolated invariant set S is one for which there exists an isolating neighborhood $N \supset S$ such that $S(t) = \mathrm{Inv}(N,\phi)(t)$.

We modify the definition autonomous isolating blocks in [21] to define nonautonomous isolating blocks. For a continuous-time nonautonomous flow ϕ given by (3.1), let Φ be the time-extended flow of ϕ, as in (3.2). For a nonautonomous set B let $B^* \subset \mathbb{R} \times X$ be the set

$$B^* = \bigcup_{t\in\mathbb{R}} \{t\} \times B(t). \tag{3.20}$$

Definition 22. We say a compact nonautonomous set B is an isolating block for ϕ if $\mathrm{Inv}_T(B,\phi) \subset \mathrm{int}\ B(t)$, where

$$\mathrm{Inv}_T(B,\phi)(t) \coloneqq \{x \in B(t) \mid \Phi([-T,T],t,x) \subset B^*\} \tag{3.21}$$

and the exit set $(B^-)^*$ is closed where

$$B^-(s) \coloneqq \{x \in B(s) \mid \Phi([0,T),s,x) \not\subset B^* \text{ for all } T > 0\} \tag{3.22}$$

and

$$(B^-)^* \coloneqq \bigcup_{s\in\mathbb{R}} \{s\} \times B^-(s). \tag{3.23}$$

3.4.1 Continuation on Riemannian Manifolds

In order to make sense of perturbations of flows, we need to know what a neighborhood of a flow is. The most common way to define a neighborhood of a flow uses its corresponding vector field.

When X is a Riemannian manifold, we can define a metric on smooth flows on X based on the vector field that ϕ generates. The flow ϕ generates a vector field $\dot{\phi}$ on the tangent space of X where $\dot{\phi}(t,x)$ is the tangent vector of the curve $\gamma : (-\epsilon,\epsilon) \to X$ at the point $\gamma(0) = x$, where $\gamma(s) = \phi(s,t,x)$.

Let $\mathcal{M}$ be the space of smooth nonautonomous flows on X. Define the nonautonomous metric $d_N^t(\phi,\psi) : \mathcal{M} \to \mathbb{R}$ by

$$d_N^t(\phi,\psi) = \sup_{x\in N(t)} ||\dot{\phi}(t,x) - \dot{\psi}(t,x)||. \tag{3.24}$$

Then given a positive function $\rho : \mathbb{R} \to \mathbb{R}^+$, the ρ-neighborhood of ϕ is:

$$B_\rho(\phi) = \{\psi \in \mathcal{M} \mid d_N^t(\phi,\psi) < \rho(t) \text{ for all } t \in \mathbb{R}\}. \tag{3.25}$$

For many applications, flows are defined by the vector field of a differential equation they solve. We quite often use the vector field to determine if a set is an isolating neighborhood or an isolating block. For example, suppose that N is a convex compact nonautonomous set with a piecewise differentiable boundary and ϕ is a smooth nonautonomous flow on a Riemannian manifold X. If the induced vector field of ϕ on $\mathbb{R} \times X$ is not tangent to the boundary of N^*, then N will be an isolating block.

Unlike isolating blocks for nonautonomous maps, an isolating block for a continuous-time nonautonomous flow is not necessarily structurally stable. If the flow is tangent to the block at a point, a small perturbation may create an internal tangency. Even for autonomous flows, isolating blocks are not necessarily structurally stable. In [10],

Conley and Easton address the structural stability of autonomous isolating blocks, proving that for a small enough perturbation, an isolating block $\tilde{N}$ can be found which is diffeomorphic to N. We conjecture that a similar stability holds for isolating blocks of nonautonomous flows, but we leave this for future work. In the next chapter, Theorem 29 addresses the structural stability of isolating blocks without tangencies.

3.4.2 Alternative Neighborhoods of Nonautonomous Flows

In the previous section, our definition of a neighborhood of a flow required that X be a Riemannian manifold. For spaces which are not Riemannian manifolds, we need alternative definitions of a neighborhood, which we will briefly outline below.

Metric Spaces

Suppose X is a metric space, and N is a nonautonomous set. We can define a nonautonomous metric $g_N^t(\phi, \psi)$ based on the distance two flows may diverge over a finite period of time:

$$g_N^t(\phi, \psi) = \sup_{x \in N(t)} \sup_{s \in [-1,1]} d_X(\phi(s,t)x, \psi(s,t)x). \tag{3.26}$$

If two nonautonomous flows ϕ and ψ have $g_N^t(\phi, \psi) < \rho(t)$ for all t, then for any finite period of time there is a limit to how far apart their trajectories may diverge. This property is also true when we use (3.24) and X is a Riemannian manifold.

Topological Spaces

If X is neither a metric space nor a manifold, a different notion for neighborhoods of flows will be required. In parts of Conley and Easton's work, they specify a few topologies on the space of autonomous flows. Because we can view a nonautonomous flow on X as a flow on $\mathbb{R} \times X$, these topologies can be easily translated for nonautonomous flows.

A nonautonomous flow ϕ can be viewed as a continuous function from $\mathbb{R} \times \mathbb{R} \times X$ to X. As such, the compact open topology on $C(\mathbb{R} \times \mathbb{R} \times X, X)$ gives us open sets for continuous functions, and the nonautonomous flows within an open set we may take to be a neighborhood of a nonautonomous flow. Conley and Easton prove that isolating neighborhoods are structurally stable in this topology on autonomous flows [10].

In Conley's monograph [9], he also describes a topology on flows using a "space of curves." If (a, b) is an open interval in $\mathbb{R}$ then a continuous function $\gamma : (a, b) \to X$ is a curve on X. If $\Gamma(X)$ is the space of all curves on X, the compact open topology can again be used to define open sets in $\Gamma(X)$. Given a starting time $t \in \mathbb{R}$ and point $x \in X$, a flow ϕ generates a curve $\gamma : (a, b) \to X$ where $\gamma(s) = \phi(s, t)x$. Then a flow can be thought of as a set of curves in $\Gamma(X)$, and flows in a neighborhood of this set in $\Gamma(X)$ we can take to be a neighborhood of the flow.

The systems we discuss in this paper are all described by differential equations in a Euclidean space, so we only use the notion of neighborhoods of nonautonomous flows on Riemannian manifolds. We leave the study of perturbations of isolating neighborhoods in nonautonomous flows on topological spaces for future work. In the next chapter, we will find explicit magnitudes for perturbations of a nonautonomous flow that do not disrupt a given isolating block. First, we present a method to prove the existence of invariant sets within certain nonautonomous isolating blocks.

3.4.3 A Ważewski Theorem for Nonautonomous Isolating Blocks

In some situations, we can find nonautonomous isolating blocks which appear, in some moving reference frame, to behave more like autonomous isolating blocks. This is often the case in rate-dependent bifurcations. We describe this moving reference frame using a monodromy function.

Definition 23. Suppose that $\xi : \mathbb{R} \times \mathbb{R} \times X \to X$ is a continuous function such that

$$\begin{aligned} \xi(t, s, N(s)) &= N(t + s) \text{ for all } t, s \in \mathbb{R} \quad \text{and} \\ \xi(t, s, N^-(s)) &= N^-(t + s) \text{ for all } t, s \in \mathbb{R}, \end{aligned} \tag{3.27}$$

where N^- is the exit set relative to the nonautonomous flow ϕ. We will call ξ a *monodromy* of N.

Theorem 24. *Let ξ be a monodromy for an isolating block N of a nonautonomous flow ϕ. Suppose that the forward invariant set of $N(t)$ relating to ϕ is empty. Then $N^-(t)$ must be a deformation retraction of $N(t)$.*

Proof. Let $x \in N(t)$ and let $\tau(x)$ be the minimum time such that $\phi(\tau(x), t)x \in N^-(t +$

$\tau(x))$. We will show that the function $h : N(t) \times [0,1] \to N^-(t)$ defined by

$$h(x,\sigma) = \xi(-\sigma \cdot \tau(x), t + \sigma \cdot \tau(x), \phi(\sigma \cdot \tau(x), t)x) \tag{3.28}$$

is a deformation retraction of $N(t)$ onto the subspace $N^-(t)$.

First, note that for all $\sigma \in [0,1]$, $\phi(\sigma \cdot \tau(x), t)x \in N(t + \sigma \cdot \tau(x))$, so $h(x,\sigma) \in N(t)$. Furthermore, since $\phi(\tau(x), t)x \in N^-(t + \tau(x))$, and ξ preserves N^-, we have $h(x,1) \in N^-(t)$. Finally, if $x \in N^-(t)$, $\tau(x) = 0$, so $h(x,\sigma) = x \in N^-(t)$ for all $\sigma \in [0,1]$.

To prove that h is a deformation retraction, we need only show that it is continuous. Since ξ and ϕ are continuous, the continuity of h relies on the continuity of τ. To show τ is continuous, we use Conley's method in [8], showing separately that it is upper and lower semi-continuous.

Suppose that $x \in N(t)$ and consider $x^* = \phi(\tau(x), t)x$. Since N is an isolating block, for any $\epsilon > 0$, we have

$$\Phi([0,\epsilon), t + \tau(x), x^*) \not\subset N^*. \tag{3.29}$$

So for some $\delta > 0$, we have $\phi(\delta, t + \tau(x))x^* \notin N(t + \tau(x) + \delta)$. Then there exists a neighborhood U of $\phi(\delta, t + \tau(x))x^*$ such that $U \not\subset N(t + \tau(x) + \delta)$. Then $V = \phi(-\delta - \tau(x), t + \tau(x) + \delta)U \cap N(t)$ is a neighborhood of x in $N(t)$ such that for any $y \in V$, $\phi(\tau(x) + \delta, t)y \notin N(t + \tau + \delta)$, so $\tau(y) < \tau(x) + \delta < \tau(x) + \epsilon$. Therefore, τ is upper semi-continuous.

Let S be the set of real numbers s such that, for any neighborhood U of x, $\tau(y) \leq s$ for some $y \in U$. Let $\bar{s} = \inf S$. If τ were not lower semi-continuous, then for any neighborhood U, there would exist $\epsilon > 0$ and $y \in U$ such that $\tau(y) \leq \tau(x) - \epsilon$. This would imply that $\bar{s} \leq \tau(x) - \epsilon$. We will show that $\bar{s} = \tau(x)$ to prove that τ is lower semi-continuous.

Let V be a neighborhood of $\Phi(\bar{s}, t, x)$ in $\mathbb{R} \times \mathbb{R}^n$. Choose $\epsilon > 0$ and a neighborhood U of x such that $\Phi((\bar{s} - \epsilon, \bar{s} + \epsilon), t, U) \subset V$. Then there exists $y \in U$ such that $\tau(y) \in (\bar{s} - \epsilon, \bar{s} + \epsilon)$, hence $\Phi(\tau(y), t, y) \in V$. Since $\Phi(\tau(y), t, y) \in (B^-)^*$ by definition, this implies that $(B^-)^* \cap V \neq \emptyset$. As V was an arbitrary neighborhood of $\Phi(\bar{s}, t, x)$ and $(B^-)^*$ is closed, it must be that $\Phi(\bar{s}, t, x) \in (B^-)^*$, implying that $\bar{s} = \tau(x)$. Thus, τ is lower semi-continuous. □

Corollary 25. *For a nonautonomous flow ϕ with an isolating block N satisfying the hypothesis of Theorem 24, the quotient space $N(t)/N^-(t)$ must be contractible.*

Proof. The function h applied to the quotient space is a deformation retraction to the point $[N^-(t)]$. □

This corollary is not necessarily a stronger statement than Ważewski's (Theorem 8), but it is slightly easier to use. As Conley states in [8], the full version of Ważewski's Theorem is rarely used in practice. Applying Ważewski's Theorem requires a careful choice of subsets of the isolating block, whereas this corollary provides a simple method of determining whether a solution exists in a given nonautonomous isolating block, based on whether it is contractible. As in Figure 3.10, for a nonautonomous system that retains its exit set in a monodromy, we can use Corollary 25 to easily prove that it has a solution remaining in N for all time.

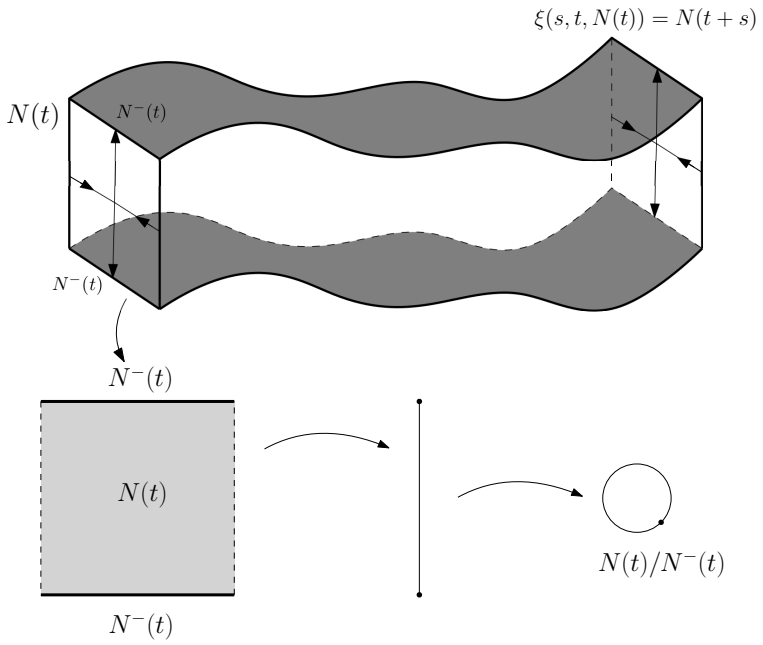

Figure 3.10: The quotient space $N(t)/N^-(t)$ is not contractible for an invariant set with the isolating block of a saddle equilibrium.

This corollary hints that we might be able to devise a Conley index for nonautonomous neighborhoods that obey a monodromy condition, which could give more information about the solution than simple existence. On the other hand, in a general

discrete nonautonomous system, we can always construct an isolating block which has its entire boundary as the exit set for $k > 0$, which indicates that such an index might not be well-defined in general. Applying other restrictions on the flow or on isolating blocks may allow for a well-defined index.

Some authors have developed a Conley index for flows on noncompact and nonautonomous spaces, but they require an admissibility condition on the flow in an isolating neighborhood, which stands in place of the compactness requirement. We are interested in nonautonomous neighborhoods which change over time, which may violate such an admissibility condition. We leave the possibility of re-framing the admissibility requirement to work with systems that have a monodromy as an avenue of future research. In the next chapter, the questions we study mainly concern the existence of invariant solutions as opposed to their topological properties. We will focus especially on attracting solutions in systems with rate-dependent forcing.

Chapter 4

Applications of Isolating Blocks in Nonautonomous and Rate-Dependent Systems

In this chapter, we apply theorems about isolating blocks to problems involving nonautonomous forcing and rate-dependent tipping. In particular, the isolating blocks give insight into how much a rate-dependent forcing function can be perturbed while expecting the same behavior from the system.

In practice, we may have a system where a parameter increases over time at an average rate which is perturbed by noise. If we can ignore the perturbations, we may find a system that is easier to analyze, which has the same qualitative behavior as the perturbed system. Our analysis of rate-dependent systems in this chapter provides a method to show when rate-dependent bifurcations arise in systems with a parameter increasing over time at an average rate perturbed by noise.

4.1 Attraction in Nonautonomous Systems

There are many notions of attraction in dynamical systems. Even for autonomous flows and maps, there are inconsistencies in the literature on how to define an attractor, and there are even more ways to describe attraction in nonautonomous flows. For an

autonomous map $f : X \to X$ on a compact space X, recall that for $U \subset X$, the omega-limit set of U is

$$\omega(U) \coloneqq \bigcap_{n\geq 0} \bigcup_{k\geq n} \mathrm{cl}(f^n(U)) \tag{4.1}$$

and we say $A \subset X$ is an attractor if there exists a neighborhood U of A such that $\omega(U) = A$. For nonautonomous sets, the omega-limit set is generally defined in a pullback sense.

Definition 26. The *pullback omega-limit set* Ω of a compact nonautonomous neighborhood N is a nonautonomous set given by

$$\Omega(t) = \bigcap_{s>0} \mathrm{cl}(\bigcup_{r>s} \phi(r, t-r)N(t-r)). \tag{4.2}$$

As $\Omega(t)$ is a nested sequence of nonempty compact sets, it is nonempty. However, the pullback omega-limit set is not necessarily an isolated invariant set. Since $\Omega(t)$ only relies on $\phi(r, t-r)$ where $t - r < t$, the $\Omega(t)$ has no dependence on the dynamics of the flow beyond time t. Furthermore, $\Omega(t)$ may not even be a subset of $N(t)$.

Rasmussen [24] provides several notions of pullback (or past) and forward (or future) attraction in nonautonomous systems. These notions are based on the asymptotic distance between nonautonomous sets. Pullback attraction has been addressed by several authors (for example, [4, 6]), but it is not necessarily related to forward attraction, and a pullback attractor may not be an invariant set. Because of this, we will not address pullback attraction, although for future research it may be worth considering in systems with rate-dependent tipping. Further research on bifurcations of pullback attractors in nonautonomous systems, such as the examples analyzed in [17], would also be worthwhile.

In autonomous systems, the attraction of equilibrium points is often described by their stability, of which there are multiple types. Recall that an equilibrium point is Lyapunov stable if there is a neighborhood N in which trajectories initiating in N remain inside it for all forward time. We provide another definition of an attracting invariant set in a nonautonomous system that is more closely related to Lyapunov stability.

Definition 27. An isolated invariant set is *trapping attracting* if it has an isolating block N which is forward invariant. That is,

$$\varphi^t(s)N(s) \subset \mathrm{int}\ N(t+s) \tag{4.3}$$

for all $t, s \in \mathbb{Z}$ (or $\mathbb{R}$ for nonautonomous flows).

This definition of attraction may not be as strong as pullback attraction; however, it suits our purposes well. We would like to be able to specify a region in a moving reference frame which has an attracting invariant set. We could then define attraction in a system with a moving parameter, where a reference frame can move along with a quasi-static equilibrium. A set which is trapping attracting is simply an isolated invariant set such that nearby solutions stay nearby.

Theorem 28. *A compact forward invariant set N holds a nonempty isolated invariant set.*

Proof. First, by definition, a forward invariant set N is an isolating block. Clearly, if $x \in N(0)$, then $\phi(t, 0)x \in N(t)$ for all $t > 0$, since N has an empty exit set. We must show that there exists a trajectory that can be extended backward in time as well. To do this, we will consider the pullback omega-limit set of N.

First, consider the discrete nonautonomous case. For $i \geq 0$, let S_i be the set in $N(0)$ defined by

$$S_i = \varphi^i(-i)N(-i) \tag{4.4}$$

and set

$$S = \bigcap_{i \geq 0} \varphi^i(-i)N(-i) = \bigcap_{i \geq 0} S_i. \tag{4.5}$$

For all i, $\varphi(-i-1)N(-i-1) \subset N(-i)$, so

$$\varphi^{i+1}(-i-1)N(-i-1) \subset \varphi^i(-i)N(-i). \tag{4.6}$$

Thus, $S_{i+1} \subset S_i$, and since each set S_i is compact, S is the intersection of a nested sequence of compact sets, hence S is nonempty. For $x \in S$, we must have $\varphi^{-i}(0)x \in N(-i)$, so the backward and forward orbit of x is in N, so x must be part of the invariant set. The same reasoning works in the continuous nonautonomous case, as for $t \in \mathbb{R}$, the intersection

$$S = \bigcap_{t \geq 0} \varphi^t(-t)N(-t) \tag{4.7}$$

will also be nonempty. □

Theorems 20 and 28 together imply that trapping attractors have structural stability. If we have an invariant set which is a trapping attractor, a perturbation of the system will still contain a forward invariant isolating block, which must contain an invariant set.

4.2 Nonautonomous Perturbations of Autonomous Systems

In this section, we will start with an autonomous system, and determine a lower bound on how much we can perturb it with nonautonomous forcing while retaining the original isolating block of the autonomous system. This is related to the concept of resilience in a system, an important factor in ecological modeling. Meyer gives a mathematical overview of resilience in ecology in [20], in which she describes several different indicators of resilience based on state variable changes and parameter changes.

Nonautonomous perturbations fall in the category of dynamic parameter changes, like those in examples of rate-dependent tipping. The way we determine bounds for these perturbations uses concepts similar to what Meyer describes as a "basin slope" in a vector field. This idea of a basin slope is also related to the concept of "intensity of attraction" introduced by McGehee in [19].

Theorem 29. *Suppose that S is an isolated invariant set with isolating block N in an autonomous system for $x \in \mathbb{R}^n$ given by*

$$\dot{x} = f(x), \tag{4.8}$$

and suppose that N has a differentiable boundary, ∂N. Assume that f is continuous and nowhere is $f(x)$ is tangent to ∂N. Let $n(x)$ be the unit normal vector at $x \in \partial N$. Define

$$M = \inf\{|f(x) \cdot n(x)| : x \in \partial N\}. \tag{4.9}$$

If $||g(x,t)|| < M$ for all t, then N is an isolating block for the nonautonomous system given by

$$\dot{x} = f(x) + g(x,t). \tag{4.10}$$

Proof. First, note that if N is a compact set then ∂N is compact and $|f(x) \cdot n(x)|$ is a continuous function of x on ∂N, so $M = \inf\{|f(x) \cdot n(x)| : x \in \partial N\}$ is positive. Consider the extended system

$$\begin{aligned} \dot{x} &= f(x) \\ \dot{t} &= 1. \end{aligned} \tag{4.11}$$

Let N^* be the constant nonautonomous set in $\mathbb{R}^n \times \mathbb{R}$ given by

$$N^* = \bigcup_{t \in \mathbb{R}} t \times N. \tag{4.12}$$

Then if x is on the boundary of N, the outward normal vector to N^* at (t, x) is $(0, n(x))$. For every point $x \in \partial N$, where $f(x) \cdot n(x) < 0$ and the vector field is pointing inward, we must have $f(x) \cdot n(x) < -M$. Then,

$$\begin{aligned} (f(x) + g(x,t)) \cdot n(x) &< f(x) \cdot n(x) + |g(x) \cdot n(x)| \\ &< f(x) \cdot n(x) + M < 0. \end{aligned} \tag{4.13}$$

Similarly, if $f(x) \cdot n(x) > 0$, we have $(f(x) + g(x,t)) \cdot n(x) > 0$. Hence, there are no points on the boundary of N^* such that the vector field $f(x) + g(x,t)$ is tangent to N^*. Thus, the nonautonomous set M with $M(t) = N$ for all t is a nonautonomous isolating block for the system 4.10. Furthermore, for each time t, the exit set $M^-(t)$ is equal to N^-, the exit set of N. □

For isolating blocks with piecewise differentiable boundaries, a similar bound can be devised. At points where the boundary is not differentiable, one should find the limiting normal vector $n_i(x)$ for each differentiable piece i, and find the minimum of $|f(x) \cdot n_i(x)|$. For continuous functions f, this bound will simply be the limit of $|f(x) \cdot n(x)|$ on one of the boundary pieces.

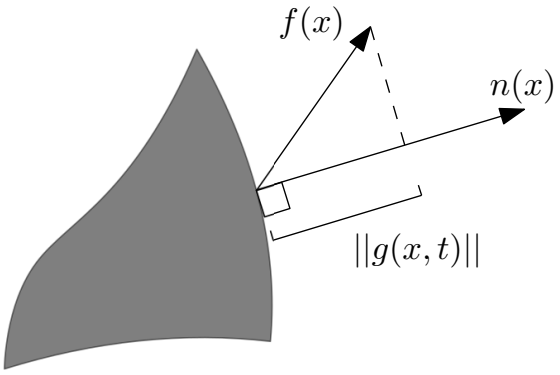

Figure 4.1: Finding a bound on a nonautonomous disturbance, $g(x,t)$.

For a trapping attracting invariant set in an autonomous system, we may introduce some nonautonomous perturbation based on Theorem 29 and retain the forward invariant isolating block. By Theorem 28, this implies that the new invariant set in N^* must be nonempty.

4.2.1 Example: Nonautonomous Forcing of a Saddle Node

Not every invariant set is an attractor or a repeller. Consider the system

$$\begin{aligned} \dot{x} &= -x(1+x^2+y^2) \\ \dot{y} &= y(1-(x^2+y^2)). \end{aligned} \tag{4.14}$$

There is a saddle equilibrium point at $(x,y)=(0,0)$, with a Jacobian of

$$J = \begin{bmatrix} -1 & 0 \\ 0 & 1 \end{bmatrix}. \tag{4.15}$$

Consider the square neighborhood of $(0,0)$ given by $[-1/2,1/2]\times[-1/2,1/2]$. For a point $(x,1/2)$ on the upper boundary of this square, the vector field is

$$f(x,y) = (-x(5/4+x^2), 1/2(3/4-x)), \tag{4.16}$$

and the normal vector $n(x,1/2)=(0,1)$, so $|f(x,1/2)\cdot n(x,12)| = 1/2(3/4-x)$, which is always positive and has a minimum of $1/8$. The other three edges of the square also have

$$\min\{|f(x,y)\cdot n(x,y)|\} = 1/8. \tag{4.17}$$

Thus, if $||\langle g_1(x,y,t), g_2(x,y,t)\rangle|| \leq 1/8$ for all $t \in \mathbb{R}$ and $(x,y) \in [-1/2,1/2]\times[-1/2,1/2]$, the nonautonomous system

$$\begin{aligned} \dot{x} &= -x(1+x^2+y^2) + g_1(x,y,t) \\ \dot{y} &= y(1-(x^2+y^2)) + g_2(x,y,t) \end{aligned} \tag{4.18}$$

has a square isolating block $N(t) = [-1/2,1/2]\times[1/2,1/2]$ for all time. Furthermore, for all t the exit set of $N(t)$ is the upper and lower sides of the square. This is a monodromy isolating block (the monodromy being the identity function) and, as depicted in Figure 3.10, the quotient space $N(t)/N^-(t)$ is not contractible. Thus, by Theorem 24, there must exist an invariant solution which is in $[-1/2,1/2]\times[1/2,1/2]$ for all time.

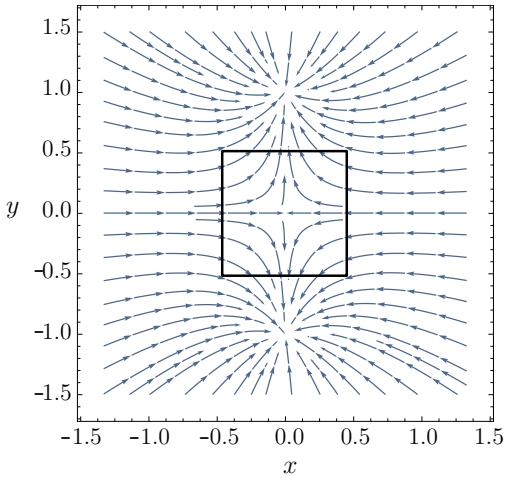

Figure 4.2: Vector field in equation 4.14, with the square isolating block.

4.3 Bounds on Rate-Dependent Tipping

Many examples of rate-dependent tipping can be found in a system of differential equations in $\mathbb{R}^n$ given by

$$\dot{x} = f(x,\lambda), \tag{4.19}$$

where $\lambda \in \mathbb{R}$. There is a point $x^*(\lambda) \in \mathbb{R}^n$ which is an attracting equilibrium for all $\lambda \in I$, for some interval I. With some knowledge of the isolating blocks for $x^*(\lambda)$, we

can find a lower bound on a rate that λ may be varied while still retaining an attracting isolating invariant set.

Suppose that $V(\lambda) \subset \mathbb{R}^n$ is a compact isolating block for $x^*(\lambda)$, and suppose that $g_\lambda(x) = 0$ defines a differentiable boundary of $V(\lambda)$, and also assume that g is differentiable with respect to λ.

Let $n(x, \lambda)$ be the inward pointing unit normal vector on the boundary of $V(\lambda)$ at x. Then $M(x, \lambda) \coloneqq f(x, \lambda) \cdot n(x, \lambda) > 0$. Consider the extended system which treats time as an independent variable:

$$\begin{aligned} x' &= f(x, \lambda(t)) \\ t' &= 1. \end{aligned} \tag{4.20}$$

Then in $\mathbb{R}^n \times \mathbb{R}$, the boundary of the set $W = \bigcup_{t\in\mathbb{R}} V(\lambda(t)) \times t$ is given by $G(x, t) = 0$ where $G(x, t) = g_\lambda(t)(x)$. Let $S_1(x, \lambda) = \operatorname{sgn}(\nabla g_\lambda(x) \cdot n_\lambda(x))$. Let $N(x, t)$ be the inward pointing normal vector to $(x, t) \in \partial W$. Let $S_2(x, t) = \operatorname{sgn}(\nabla G(x, t) \cdot N(x, t))$. Then,

$$n_\lambda(x) = S_1(x, \lambda)\frac{\nabla g_\lambda(x)}{||\nabla g_\lambda(x)||} \quad \text{and} \tag{4.21}$$

$$N(x, t) = S_2(x, t)\frac{\nabla G(x, t)}{||\nabla G(x, t)||}. \tag{4.22}$$

If we project $N(x, t)$ onto just its x component and renormalize, we get $n_{\lambda(t)}(x)$. The same projection and renormalization turns $S_2(x, t)\frac{\nabla G(x,t)}{||\nabla G(x,t)||}$ into $S_2(x, t)\frac{\nabla g_{\lambda(t)}(x)}{||\nabla g_{\lambda(t)}(x)||}$. Therefore, $S_2(x, t) = S_1(x, \lambda(t))$. Thus,

$$\begin{aligned} N(x, t) &= \frac{1}{C}\langle n(x, \lambda(t)), S\frac{d}{dt}G(x, t)\rangle \\ &= \frac{1}{C}\langle n(x, \lambda(t)), S\frac{d}{dt}\lambda(t)\frac{\partial}{\partial\lambda}g_\lambda(x)\rangle, \end{aligned} \tag{4.23}$$

where $C = ||\langle n(x, \lambda(t)), S\frac{d}{dt}G(x, t)\rangle||$ and $S = \operatorname{sgn}(\nabla g_{\lambda(t)}(x) \cdot n_{\lambda(t)}(x))$. Then to determine if the vector field of the system (4.20) points inward we check the sign of

$$\langle f(x, \lambda(t)), 1\rangle \cdot \frac{1}{C}\langle n(x, \lambda(t)), S\frac{d}{dt}\lambda(t)\frac{\partial}{\partial\lambda}g_\lambda(x)\rangle = \frac{1}{C}\big(M + S\frac{d}{dt}\lambda(t)\frac{\partial}{\partial\lambda}g_\lambda(x)\big). \tag{4.24}$$

The vector field of the nonautonomous flow points inward if (4.24) is greater than 0, or when

$$M(x, \lambda(t)) > -S\frac{d}{dt}\lambda(t)\frac{\partial}{\partial\lambda}g_\lambda(x). \tag{4.25}$$

This implies the following theorem:

Theorem 30. *Given the system (4.19) and forward invariant isolating block $V(\lambda)$ for the quasi-static equilibrium $x^*(\lambda)$, with normal vector $n(x,\lambda)$, let*

$$M = \inf_{\lambda\in\Lambda} \inf_{x\in\partial V(\lambda)} |f(x,\lambda)\cdot n(x,\lambda)|. \tag{4.26}$$

Then if, for all t,

$$|\frac{d}{dt}\lambda(t)\frac{\partial}{\partial\lambda}g_\lambda(x)| < M, \tag{4.27}$$

the nonautonomous system (4.20) will have an isolated invariant set with the forward invariant isolating block W where $W(t) = V(\lambda(t))$.

If the neighborhood $V(\lambda)$ moves constantly with respect to $x^*(\lambda)$, then we can replace $\frac{\partial}{\partial\lambda}g_\lambda(x)$ by $||\frac{\partial}{\partial\lambda}x^*(\lambda)||$ in (4.27). Theorem 30 gives only a crude lower bound on the tipping point for the rate, r, but it can be useful, as we will show in a few examples. The bound given by (4.25) could be used to give a tighter result.

4.3.1 Example: Saddle Bifurcation in 1D System

The first example of rate-dependent tipping comes from the paper by Ashwin et al. [2]. It is a one dimensional saddle node which is drifting over time:

$$\dot{x} = (x+\lambda)^2 - \mu. \tag{4.28}$$

Fixing $\lambda\in\mathbb{R}$, the point $x^*(\lambda) = -1-\lambda$ is an attracting equilibrium.

There is an isolating neighborhood of $x^*(\lambda)$ given by $[-\sqrt{2\mu}-\lambda, -\lambda]$. Note that on the boundary of this interval,

$$f(-\sqrt{2\mu}-\lambda) = \mu \quad \text{and} \quad f(-\lambda) = -\mu. \tag{4.29}$$

So both vectors on the boundary point inwards, and they have a magnitude of μ. Therefore, if $\lambda(t) = rt + c$, then

$$\left|\frac{d\lambda}{dt}\frac{d}{d\lambda}x^*(\lambda)\right| = |r(-1)| = r. \tag{4.30}$$

Thus, if $r < \mu$, there exists an invariant solution $x(t)\in[-\sqrt{2\mu}-\lambda(t), -\lambda(t)]$. Ashwin et al. give a more general bound based on the initial conditions of x and λ; however, we do find the same bound guaranteeing that a solution exists that tracks $x^*(\lambda(t))$.

4.3.2 Example: Hopf Normal Form

The second example of rate-dependent tipping also comes from Ashwin et al. and is in two dimensions:

$$\begin{aligned}\dot{x} &= -(x-\lambda) - \omega y + (x-\lambda)((x-\lambda)^2 + y^2) \\ \dot{y} &= \omega(x-\lambda) - y + y((x-\lambda)^2 + y^2).\end{aligned} \tag{4.31}$$

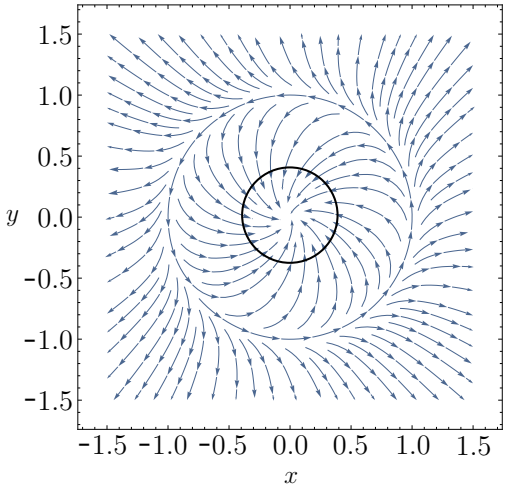

Figure 4.3: Vector field in equation 4.31 when $\lambda = 0$, and a circular isolating block for the stable equilibrium.

This system has a quasi-static equilibrium at $(x, y)^*(\lambda) = (\lambda, 0)$. For any $0 < r < 1$, a disc of radius r centered at $(x, y)^*$ is a forward invariant isolating block for $(x, y)^*$. We may calculate the bound, M_r, given by Theorem 30 for each circle of radius r. Since the vector field moves constantly with λ, we can calculate the bound assuming that $\lambda = 0$. For a point (x, y) on the boundary of the circle $x^2 + y^2 = r^2$, the outward normal vector is $\langle x, y\rangle/r$. Thus,

$$\begin{aligned}M_r = |f(x,y) \cdot \langle x, y\rangle/r| &= |(x(-x - \omega y + x(r^2)) + y(\omega x - y + y(r^2)))/r| \\ &= |-x^2/r + x^2 r - y^2/r + y^2 r| \\ &= |r^3 - r| \\ &= r(1 - r^2).\end{aligned} \tag{4.32}$$

This has a maximum at $r = \sqrt{1/3}$, where $M_r = \frac{2}{3\sqrt{3}}$. Since

$$\left|\left|\frac{\partial}{\partial\lambda}(x,y)^*(\lambda)\right|\right| = 1, \tag{4.33}$$

Theorem 30 implies that if $\frac{d}{dt}\lambda(t) < \frac{2}{3\sqrt{3}}$, the system will not tip.

Note that this bound does not depend on ω at all. Ashwin et al. give a stricter bound based on ω, and our bound matches theirs only when $\omega = 0$. The advantage of our method is that it is relatively simple.

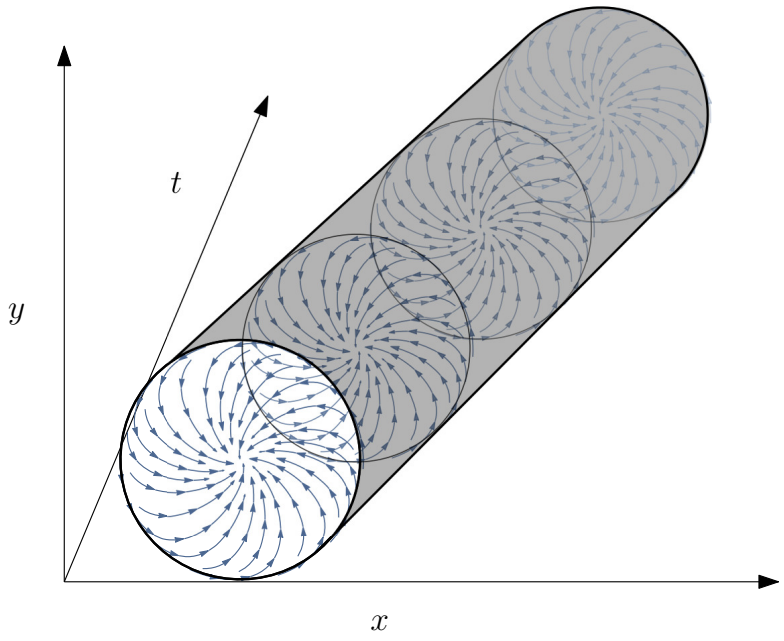

Figure 4.4: The vector field moving over time. As time increases, the vector field moves in the positive x direction.

4.3.3 The Rate-Dependent Hopf Bifurcation, Revisited

In the main example of Chapter 2 (equation 2.2), for $r > r_c$, we found a spiraling invariant set which corresponded to a stable limit cycle in the autonomous system in (x, v) coordinates (2.6). As we know for autonomous systems, this implies we can find a trapping attracting isolating block $\bar{B}$ in the (x, v) plane that surrounds the limit cycle.

In the system (2.2) in (x, y) coordinates, which is not co-moving, $\bar{B}$ corresponds to a nonautonomous isolating block B, where $B(t) = \{(x, y)|(x, y + rt) \in \bar{B}\}$.

We also know from Theorem 29 that we can perturb the (x, v) system with nonautonomous forcing $g(x, y, t)$ bounded in magnitude by some constant M, and $\bar{B}$ will remain a isolating block which is still trapping attracting. For example, if we alter (2.6) with the perturbation $\rho(t)$ to create the system given by

$$\begin{aligned} \epsilon\dot{x} &= v + x(x-1) + \rho(t) \\ \dot{v} &= -\sum_{i=1}^{N} x^i + r \end{aligned} \tag{4.34}$$

then $\bar{B}$ will still be trapping attracting if $|\rho(t)/\epsilon| < M$. Replacing v with $y + rt$, we have a system in (x, y) where B is a trapping attracting nonautonomous isolating block:

$$\begin{aligned} \epsilon\dot{x} &= y + rt + \rho(t) + x(x-1) \\ \dot{y} &= -\sum_{i=1}^{N} x^i. \end{aligned} \tag{4.35}$$

Thus, the nonautonomous isolating block B still contains an invariant solution in the system with a perturbed forcing:

$$\begin{aligned} \epsilon\dot{x} &= y + \tilde{\lambda}(t) + x(x-1) \\ \dot{y} &= -\sum_{i=1}^{N} x^i \\ \tilde{\lambda}(t) &= rt + \rho(t). \end{aligned} \tag{4.36}$$

Chapter 5

Rate-Dependent Tipping in Maps

Rate-dependent tipping is a relatively new concept. It has only been analyzed in a limited number of settings, and relatively few of types of forcing functions that cause it have been analyzed. Ashwin et al. have mainly analyzed rate-dependent tipping in ordinary differential equations, and Ritchie and Sieber [25, 26] have looked at the interplay between rate-dependent tipping and noise in stochastic differential equations.

In the previous chapters, we used basic concepts of isolating blocks to analyze examples of rate-dependent tipping in systems of differential equations. A good portion of the theory we examined dealt with discrete isolating blocks in systems of nonautonomous maps. It seems natural, then, to consider extending the idea of rate-dependent tipping to discrete maps. Here we will formulate the idea of rate-dependent bifurcations in time-dependent maps, and apply it to a few examples which demonstrate the rich complexity of rate-dependent bifurcations.

5.1 Defining Rate-Dependent Tipping in Maps

Begin with a family of autonomous maps $f(\lambda, \cdot) : X \to X$ on a metric space, X, that depends on a parameter λ. A fixed point $x^* \in X$ is one such that $x^* = f(\lambda, x^*)$. Recall that a fixed point is *Lyapunov stable* if there exists a radius δ such that for any $\epsilon < \delta$, $|x^* - x| < \epsilon$ implies $|x^* - f(x, \lambda)| < \epsilon$. We say a fixed point is *asymptotically stable* if there exists $\epsilon > 0$ such that $|x^* - x| < \epsilon$ implies $\lim_{n\to\infty} |x^* - f^n(x, \lambda)| = 0$. If $x^*(\lambda)$ is Lyapunov and asympotically stable, there is an isolating block N_λ of $x^*(\lambda)$ which can

be chosen to satisfy $f(\lambda, N_\lambda) \subset \text{int } N_\lambda$.

Suppose that for each value of $\lambda \in \Lambda$ we have $x^*(\lambda)$ such that

1. $x^*(\lambda)$ is a fixed point for $f(\cdot, \lambda)$
2. $x^*(\lambda)$ is Lyapunov stable and asymptotically stable
3. $x^*(\lambda)$ depends continuously on λ.

Then if λ depends on time, we will call $x^*(\lambda)$ a quasi-static equilibrium. Consider a continuous time-varying parameter function $\lambda : \mathbb{R} \to \Lambda$ and the nonautonomous map $g : \mathbb{Z} \times X \to X$ where for some $r > 0$:

$$g(k, x) = f(\lambda(rk), x). \tag{5.1}$$

An orbit of this is a sequence $\{..., x_{-1}, x_0, x_1, ...\}$ such that

$$x_{k+1} = f(\lambda(rk), x_k). \tag{5.2}$$

We say that $\{..., x_{-1}, x_0, x_1, ...\}$ is a *tracking* orbit if x_k stays within some prescribed neighborhood of the $x^*(\lambda(rk))$.

Theorem 31. *Suppose that Λ is a compact metric space, $\lambda : \mathbb{R} \to \Lambda$ is Lipshitz continuous, and $f : \Lambda \times X \to X$. Further, suppose that for each value of $\lambda \in \Lambda$, there is a stable equilibrium, $x^*(\lambda)$, of the map $f(\lambda, \cdot)$, and a trapping attracting isolating block N_λ which depends continuously on λ. Then for some rate $r > 0$, there exists an orbit $\{x_k\}$ of $\tilde{f}(k, x) \coloneqq f(\lambda(rk), x)$ which tracks $x^*(\lambda(rk))$.*

Proof. Since $f(\lambda, N_\lambda) \subset \text{int } N_\lambda$, and N_λ depends continuously on λ, there exists a neighborhood U of λ such that $f(\lambda, N_\lambda) \subset \text{int } N_\psi$ for $\psi \in U$. Define the distance

$$D_\lambda = \sup\{D | f(\lambda, N_\lambda) \subset \text{int } N_\psi \text{ for all } \psi \text{ such that } d(\lambda, \psi) < D\} \tag{5.3}$$

where d is the metric on Λ. Then $D_\lambda > 0$, and since f is continuous, D_λ is also continuous. Let $\bar{D} = \inf_{\lambda \in \Lambda} D_\lambda$. Since D_λ is continuous and Λ is compact, $\bar{D} > 0$. Since λ is globally Lipshitz, there exists L such that

$$d(\lambda(x), \lambda(y)) \leq L|x - y| \quad \text{for all} \quad x, y \in \mathbb{R}. \tag{5.4}$$

Let $r = \bar{D}/L$, and let M be the nonautonomous neighborhood of $x^*(\lambda(rk))$, where $M(k) = N_{\lambda(rk)}$. Then $|rk - r(k+1)| = r = \bar{D}/L$, so $d(\lambda(rk), \lambda(r(k+1))) \leq \bar{D}$ for all $k \in \mathbb{Z}$. Therefore

$$f(\lambda(rk), N_{\lambda(rk)}) \subset \text{int } N_{\lambda(r(k+1))} \tag{5.5}$$

implying that M is a trapping attracting isolating block, as

$$\tilde{f}(k, M(k)) \subset \text{int } M(k+1). \tag{5.6}$$

Theorem 28 implies that there is a nonempty invariant set in M, an orbit which stays within the neighborhood of $x^*(\lambda(rk))$. □

In practice, these isolating neighborhoods and rate r may be difficult to compute analytically. In some cases, reductions such as those found in the examples in Chapter 2 may be available to analyze the problem.

5.2 Example: Steadily Drifting Linear System

Let A be a two-dimensional square matrix with eigenvalues E_1, E_2 such that $|E_i| < 1$. Consider the system

$$f(\begin{pmatrix} x \\ y \end{pmatrix}, \lambda) = A \begin{pmatrix} x - \lambda \\ y \end{pmatrix} + \begin{pmatrix} \lambda \\ 0 \end{pmatrix}. \tag{5.7}$$

For each λ, the point $(x, y) = (\lambda, 0)$ is a stable equilibrium. If $\lambda = rk$ changes linearly over time at a rate r, we have a nonautonomous system given by the map

$$g(\begin{pmatrix} x \\ y \end{pmatrix}, k) = A \begin{pmatrix} x - rk \\ y \end{pmatrix} + \begin{pmatrix} rk \\ 0 \end{pmatrix} \tag{5.8}$$

with a QSE at $(x, y)^* = (rk, 0)$. An example of an orbit of this nonautonomous system is demonstrated in Figure 5.1. Then $\bar{x}_k = x_k - rk$ gives the difference between the x-coordinate of the state and the QSE at time k. Since $\bar{x}_{k+1} = x_{k+1} - r(k+1)$, an orbit in $(\bar{x}, y)$ coordinates satisfies

$$\begin{aligned} \begin{pmatrix} \bar{x}_{k+1} \\ y_{k+1} \end{pmatrix} &= A \begin{pmatrix} x_k - rk \\ y \end{pmatrix} + \begin{pmatrix} rk \\ 0 \end{pmatrix} - \begin{pmatrix} r(k+1) \\ 0 \end{pmatrix} \\ &= A \begin{pmatrix} \bar{x}_k \\ y \end{pmatrix} - \begin{pmatrix} r \\ 0 \end{pmatrix}. \end{aligned} \tag{5.9}$$

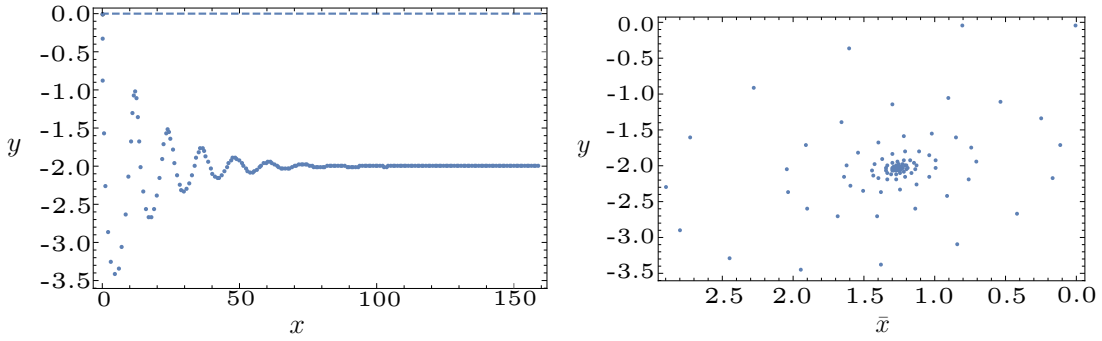

Figure 5.1: Left: The moving QSE (dashed line), and an orbit in the nonautonomous linear system (5.8) with $A = \begin{bmatrix} 1 & -2/5 \\ 2/5 & 3/4 \end{bmatrix}$ and $r = 0.8$, for $0 \leq k \leq 200$. Right: the same orbit in the corresponding lag system (5.9) as it approaches equilibrium.

This autonomous linear system has a stable fixed point at

$$(A - I)^{-1} \begin{pmatrix} r \\ 0 \end{pmatrix} \tag{5.10}$$

which implies that the state (x_k, y_k) will follow the QSE at a fixed distance asymptotically no matter the rate r, although this distance is an increasing function of r.

5.3 Example: Steadily Drifting Logistic Map

In the second example we again examine a steadily drifting equilibrium, this time in a quadratic system. Consider the map

$$f(\lambda, x) = \alpha(x + \lambda)(1 - (x + \lambda)) - \lambda. \tag{5.11}$$

There are two equilibrium points, at $x = -\lambda$ and $x = 1 - \frac{1}{\alpha} - \lambda$, and

$$f'(x) = \alpha(1 - 2\lambda - 2x) \tag{5.12}$$

so if $1 < \alpha < 3$, the equilibrium $x^* = 1 - \frac{1}{\alpha} - \lambda$ is stable. If we force λ linearly over time, so that $\lambda = rk$, we have the nonautonomous system

$$g(k, x) = \alpha(x + rk)(1 - (x + rk)) - rk \tag{5.13}$$

and a QSE at $x^* = 1 - \frac{1}{\alpha} - rk$. If we set $\bar{x}_k = x_k - (1 - \frac{1}{\alpha} - rk)$, so that it is the lag between the solution and the QSE, we find

$$\begin{aligned} \bar{x}_{k+1} &= x_{k+1} - 1 + \frac{1}{\alpha} + r(k+1) \\ &= \alpha(x_k + rk)(1 - (x_k + rk)) - rk - 1 + \frac{1}{\alpha} + r(k+1) \\ &= \alpha(\bar{x}_k + 1 - \frac{1}{\alpha})(\frac{1}{\alpha} - \bar{x}_k)) - 1 + \frac{1}{\alpha} + r \\ &= \alpha\bar{x}_k^2 + (\alpha - 2)\bar{x}_k + r. \end{aligned} \tag{5.14}$$

So the orbit of $\bar{x}$ is governed by the equation

$$h(\bar{x}) = \alpha\bar{x}^2 + (\alpha - 2)\bar{x} + r. \tag{5.15}$$

This map has two fixed points at

$$\bar{x}_\pm = \frac{1 - \alpha \pm \sqrt{1 + \alpha(\alpha - 2 + 4r)}}{2\alpha}. \tag{5.16}$$

Then, testing the stability of the fixed points, we have

$$\begin{aligned} h'(\bar{x}) &= 2 - \alpha - 2\bar{x}\alpha \\ h'(\bar{x}_\pm) &= 1 \mp \sqrt{1 + \alpha(\alpha - 2 + 4r)}. \end{aligned} \tag{5.17}$$

Thus, as $|h'(\bar{x}_-)| > 1$, the fixed point $\bar{x}_-$ is unstable; however, $\bar{x}_+$ is a stable fixed point when $\alpha(\alpha - 2 + 4r) < 0$. At this rate, the solution tracks the QSE at a steady distance.

For some values A, B and C (where $C > 0$), there exists a linear change of coordinates $y = A\bar{x} + B$ which transforms the quadratic polynomial in (5.15) so that

$$\begin{aligned} y_{k+1} &= A\bar{x}_{k+1} + B \\ &= A(\alpha\bar{x}_k^2 + (\alpha - 2)x_k + r) + B \\ &= Cy_k(1 - y_k). \end{aligned} \tag{5.18}$$

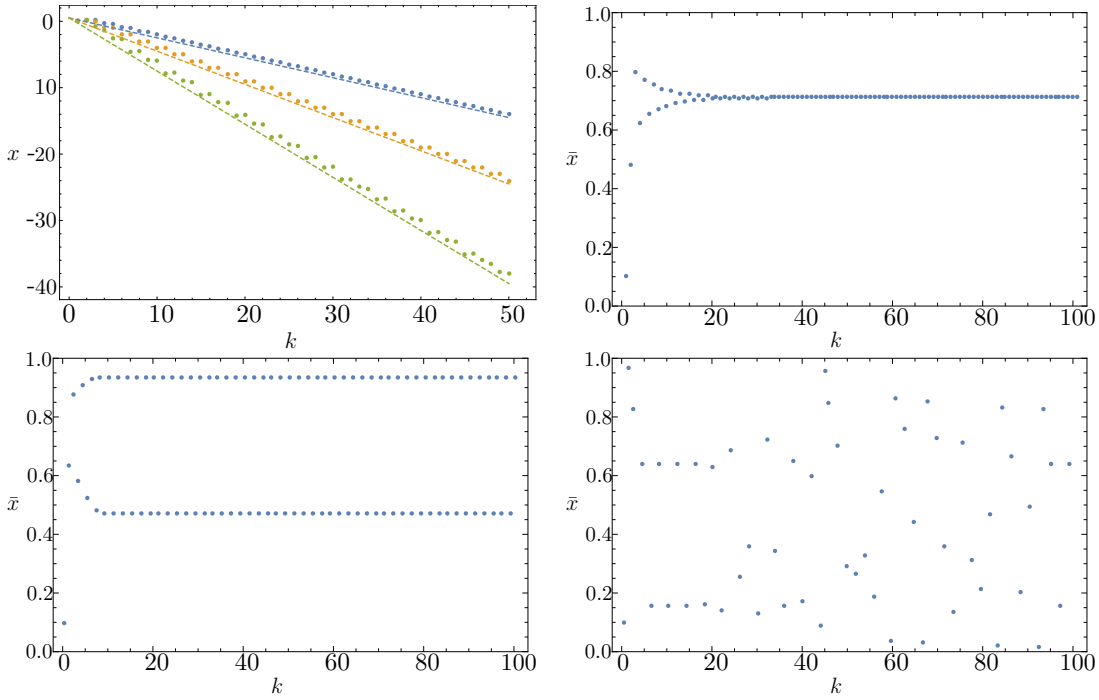

Figure 5.2: Demonstration of tracking for $\alpha = 2$ and three rates, $r = .3$ (top right), $r = .5$ (bottom left), and $r = .8$ (bottom right). These show the three different tracking behaviors (steady, periodic, and chaotic, respectively). The top left plot shows the three orbits (dots) following the QSE (dashed lines) for all three rates.

The values of A, B and C are

$$\begin{aligned} A &= \frac{\alpha}{1+\sqrt{1+Z}} \\ B &= \frac{2-\alpha+Z+(\alpha-2)\sqrt{1+Z}}{2Z} \\ C &= 1+\sqrt{1+Z} \end{aligned} \tag{5.19}$$

where $Z = \alpha(\alpha - 2 + 4r)$. The map

$$y_{k+1} = Cy_k(1-y_k) \tag{5.20}$$

is the well-known logistic equation, whose behavior depends on the value of C. For $1 < C < 3$, there is a stable fixed point. For $3 < C < 1+\sqrt{6}$, orbits approach a period-two oscillation. As C increases from $1+\sqrt{6}$ to 4, there continue to be period-doubling

bifurcations, and a descent into chaotic orbits. For $C > 4$, orbits diverge. This means that the behavior of $\bar{x}$ depends on r in the following way:

$-1 < \alpha(\alpha - 2 + 4r) < 3$	Stable Tracking
$3 < \alpha(\alpha - 2 + 4r) < 5$	Period-2 Tracking
$5 < \alpha(\alpha - 2 + 4r) < 8$	Periodic or Chaotic Tracking
$8 < \alpha(\alpha - 2 + 4r)$	No Tracking

Table 5.1: Ranges of values for α and r for stable, periodic, chaotic tracking, or no tracking at all in equation (5.13).

Examples of the three tracking behaviors are demonstrated in Figure 5.2.

These examples are quite simple, but they show how complicated behavior can arise in steadily drifting maps. As the second example shows, rate-dependent bifurcation may have more structure than a simple transition from tracking to tipping. The tracking behavior can have periodic oscillations, analogous to the spiraling behavior in the rate-dependent bifurcations in Chapter 2. The solution can also track the QSE in a chaotic manner. We have only touched on the idea of rate-dependent bifurcations in maps. We believe one could expand on this idea in many ways: for example, examining maps in higher dimensions, in stochastic systems, or with alternate forcing functions.

Chapter 6

Conclusion

Simple examples can provide insight into the complex behavior that solutions exhibit in rate-dependent systems. In this work, we have examined several systems in which a type of Hopf bifurcation occurs when a parameter is forced at a high enough rate, causing solutions to spiral around a QSE. This suggests that a natural periodic behavior could arise in real-world systems when a parameter is changing over time, even if there seems to be an attracting equilibrium for every value of the parameter. We found this behavior in a simple model of consumer and resource densities in an ecosystem in which the resource growth rate is declining over time.

We developed a concept of nonautonomous isolating blocks to better understand this kind of nonautonomous bifurcation. We used isolating blocks to prove the existence of solutions existing inside a moving region in state-space, as well as to prove that spiraling solutions in rate-dependent systems may occur when a parameter changes at an average rate with some amount of noise. By considering the strength of the vector field on the boundary of an isolating block, we also determined a crude lower bound on a critical value for rate-dependent tipping.

For autonomous systems, topological properties of isolating blocks and corresponding exit sets the were used to develop the Conley index, which provides more information about invariant solutions inside. It is possible that a similar index could be developed for isolating blocks which satisfy the monodromy requirement in Theorem 24. This could help to classify types of bifurcations of rate-dependent systems inside regions that move along with a QSE.

There is still a great deal of work to do to understand rate-dependent systems. This includes further study of rate-dependent bifurcations in stochastic differential equations and in time-dependent maps. In this work, we considered steadily drifting parameters, but there is a wide array of forcing functions still to consider (e.g. a single pulse, a periodic function, or a logistic shift). Numerical methods for finding isolating blocks in nonautonomous systems may be helpful for practical applications and a topic for future applied research.

There is significant interest in tipping points in climate science, ecology, and other areas of science. We expect that rate-dependent bifurcations like the ones examined in this work occur in many real-world systems. We have shown how oscillatory and even chaotic behavior can arise in simple systems and may be present in more complex systems, even in the presence of noise. Observations of this sort of characteristic behavior could help in determining when a tipping event will occur.

References

[1] P. Ashwin, C. Perryman, and S. Wieczorek. Parameter shifts for nonautonomous systems in low dimension: bifurcation- and rate-induced tipping. *Nonlinearity*, 30(6):2185–2210, 2017.

[2] P. Ashwin, S. Wieczorek, R. Vitolo, and P. Cox. Tipping points in open systems: bifurction, noise-induced, and rate-dependent examples in the climate system. *Phil. Trans. R. Soc. A*, 370:1166–1184, 2012.

[3] E. Benoit, J. L. Callot, F. Diener, and M. Diener. Chasse au canard (premiére partie). *Collectanea Mathematica*, 32(1):37–74, 1981.

[4] T. Caraballo, J. C. Jara, J. A. Langa, and Z. Liu. Morse decomposition of attractors for non-autonomous dynamical systems. *Advanced Nonlinear Studies*, 13:309–329, 2015.

[5] A. Carvalho, J. A. Langa, and J. C. Robinson. *Attractors for infinite-dimensional non-autonomous dynamical systems*, volume 182 of *Applied Mathematical Sciences*. Springer, 2013.

[6] D. N. Cheban, P. E. Kloeden, and B. Schmalfuss. The relationship between pullback, forward and global attractors of nonautonomous dynamical systems. *Nonlinear Dynamics and Systems Theory*, 2(2):125–144, 2002.

[7] S. Chow, C. Li, and D. Wang. *Normal Forms and Bifurcation of Planar Vector Fields*. Cambridge University Press, 2013.

[8] C. Conley. A new statement of Ważewski's theorem and an example. In *Ordinary and Partial Differential Equations,* (W. Everitt, editor), volume 564 of *Lecture Notes in Math*, pages 61–71. Springer-Verlag, Berlin, 1976.

[9] C. Conley. Isolated invariant sets and the Morse index. In *CBMS Regional Conference Series in Mathematics*, number 38. Amer. Math. Soc., Providence, 1978.

[10] C. Conley and R. Easton. Isolated invariant sets and isolating blocks. *Trans. Amer. Math. Soc.*, 158(1):35–61, 1971.

[11] M. Diener. The canard unchained or how fast/slow dynamical systems bifurcate. *The Mathematical Intelligencer*, 6(3):38–49, 1984.

[12] R. Easton. On the existence of invariant sets inside a submanifold convex to a flow. *J. Differential Equations*, 7(1):54–68, 1970.

[13] J. Franks and D. Richeson. Shift equivalence and the Conley index. *Trans. Amer. Math. Soc.*, 352(7):3305–3322, 2000.

[14] J. Guckenheimer, K. Hoffman, and W. Weckesser. The forced van der Pol equation I: the slow flow and its bifurcations. *SIAM J. Applied Dynamical Systems*, 2(1):1–35, 2003.

[15] J. Hahn. Hopf bifurcations in fast/slow systems with rate-dependent tipping. *arXiv:1610.09418*, 2016.

[16] A. Jänig. A non-autonomous conley index. *J. Fixed Point Theory Appl.*, 19(3):1825–1870, 2017.

[17] J. H. Li, F. X. Ye, H. Qian, and S. Huang. Time dependent saddle node bifurcation: breaking time and the point of no return in a non-autonomous model of critical transitions. *arXiv:1611.09542*, 2017.

[18] Z. Liu. Conley index for random dynamical systems. *J. Differential Equations*, 244(7):1603–1628, 2008.

[19] R. P. McGehee. Some metric properties of attractors with applications to computer simulations of dynamical systems. Unpublished Manuscript, 1988.

[20] K. Meyer. A mathematical review of resilience in ecology. *Natural Resource Modeling*, 29(3):339–352, 2016.

[21] K. Mischaikow and M. Mrozek. Conley index theory. In *Handbook of Dynamical Systems, Volume 2* (B. Fiedler, editor), pages 393–460. Elsevier, 2002.

[22] C. Perryman. *How fast is too fast? Rate-induced bifurcations in multiple time-scale systems*. PhD thesis, University of Exeter, 2015.

[23] J. Rankin, B. Desroches, B. Krauskopf, and M. Lowenberg. Canard cycles in aircraft ground dynamics. *Nonlinear Dynamics*, 66:681–688, 2011.

[24] M. Rasmussen. *Attractivity and Bifurcation for Nonautonomous Dynamical Systems*, volume 1907 of *Lecture Notes in Mathematics*. Springer, 2007.

[25] P. Ritchie and J. Sieber. Early-warning indicators for rate-induced tipping. *Chaos*, 26:093116, 2016.

[26] P. Ritchie and J. Sieber. Probability of noise- and rate-induced tipping. *Phys. Rev. E*, 95:052209, 2017.

[27] M. Scheffer, E. H. van Nes, M. Holmgren, and T. Hughes. Pulse-driven loss of top-down control: the critical-rate hypothesis. *Ecosystems*, 11:226–237, 2008.

[28] K. Siteur, M. B. Eppinga, A. Doelman, E. Siero, and M. Rietkerk. Ecosystems off track: rate-induced critical transitions in ecological models. *Oikos*, 125(12):1689–1699, 2016.

[29] R. Srzednicki. Ważewski method and Conley index. In *Handbook of Differential Equations: Ordinary Differential Equations, Volume 1* (A. Cañada, P. Drábek, and A. Fonda, editors), pages 591–684. Elsevier, 2004.

[30] P. Szmolyan and M. Weschelberger. Canards in $\mathbb{R}^3$. *J. Differential Equations*, 177:419–453, 2001.

[31] T. Ważewski. Sur un principe topologique de l'examen de l'allure asymptotique des intégrales des équations différentielles ordinaires. *Ann. Soc. Polon. Math.*, 20:279–313, 1947.

[32] S. Wieczorek, P. Ashwin, C. M. Luke, and P. M. Cox. Excitability in ramped systems: the compost bomb instability. *Proc. R. Soc. A*, 467:1243–1269, 2011.